Sensitivity of photochemical surface ozone formation regimes to emissions and meteorology in India

Gopalakrishna Pillai Gopikrishnan[1,2], Daniel M. Westervelt[2] and Jayanarayanan Kuttippurath[1]

[1]CORAL, Indian Institute of Technology Kharagpur, Kharagpur–721302, India.
[2]Lamont-Doherty Earth Observatory, Columbia University, New York - 10964, NY, USA

Correspondence to:
Daniel M. Westervelt (*danielmw@ldeo.columbia.edu*)
Jayanarayanan Kuttippurath (*jayan@coral.iitkgp.ac.in*)

Abstract. Atmospheric aerosols significantly contribute to air pollution and influence atmospheric chemistry, impacting air quality and public health. Decrease in aerosols can hinder the radical uptake sink of HO_2, and thus increase NO_x and OH, and subsequently increase ozone levels. This study investigates the seasonal variations of PM_{10} and aerosol surface area and their effect on surface ozone levels in India, using the GEOS-Chem Chemical Transport Model for the years 2018 and 2022, two years with high and low simulated PM_{10} concentrations, respectively. The results reveal substantial seasonal variations in PM_{10} and aerosol surface area. In winter (DJF), higher PM_{10} and aerosol surface area in the Indo-Gangetic Plain (IGP) and western Central India (CI) result from biomass burning and industrial activity, while coastal regions show lower aerosol surface area. A decrease in aerosol surface area is seen during the pre-monsoon (March-April-May; MAM) and monsoon (June-July-August-Septmember; JJAS), followed by an increase in the post-monsoon (ON) season. As a result, aerosol-induced HO_2 uptake during winter and post-monsoon suppress surface ozone by approximately 5–10 μg/m³ in 2022 when compared to that of 2018. In contrast, during monsoon in 2022, the decrease in aerosol surface area caused an ozone increase of 5–7.5 μg/m³ when compared to that of 2018. On average, this increase in surface ozone due to the decrease in aerosols can be mitigated by reducing anthropogenic NO_x emissions by about 25–50%. Thus, we recommend integrated strategies addressing aerosols, precursor emissions and regional meteorology to combat ozone pollution.

1. Introduction

In recent decades, surface ozone (O_3) has gained significant research attention due to its role as a transient (ranging from a few hours to a few weeks) secondary pollutant and its detrimental impacts on human health and agricultural yield (e.g., Mills et al. 2007; Avnery et al. 2011; Rathore et al., 2023; Gopikrishnan and Kuttippurath, 2024). It is an important trace gas in tropospheric chemistry, facilitating oxidation processes as the principal source of hydroxyl radicals (OH) (Logan, 1985) while also involved in chemical reactions with various organic molecules (Anderson, 2007). Ozone in the troposphere is a secondary pollutant generated via photochemical reactions that involve carbon monoxide (CO) and volatile organic compounds (VOCs) together with nitrogen oxides (NO_x = $NO + NO_2$), recognised as ozone precursors (Crutzen 1995; Gopikrishnan et al., 2022). However, these processes are dependent on solar radiation, with the reaction rate often peaking during summer months.

The formation dynamics of surface ozone is greatly affected by the presence of precursors such as NO_x and VOCs, resulting in NO_x-limited and VOC-limited regimes (Fiore et al., 2002; Lu et al., 2019). In the NO_x-limited regime, the concentration of NO_x is low compared to VOCs, implying that increasing NO_x levels can promote further ozone generation due to inadequate NO_x to completely react with VOCs. In a VOC-limited regime, the availability of VOCs is restricted, and further VOC emissions can significantly enhance ozone formation, whereas additional NOx may have less effect on ozone formation. Nevertheless, these regimes are significantly affected by local emission sources, atmospheric chemistry and climatic conditions. For instance, aerosols can influence these regimes by modifying the concentration of hydroxyl (OH) and hydroperoxyl (HO_2) radicals, affecting the equilibrium between NO_x and VOCs and eventually determining the rate and extent of ozone generation in different locations (Jacob et al., 2005; Feng et al., 2016; Wang et al., 2018; Li et al., 2019; Ivatt et al., 2022; Gopikrishnan et al., 2025).

Previous studies based on ground-based measurements from urban centers and industrial sites have shown substantial decrease in the particulate matter in the Indian cities post the implementation of National Clean Air Programme (NCAP), which primarily targets reducing the city-level PM pollution by 20–30% in 131 cities when compared to that of 2017–18. Gopikrishnan and Kuttippurath (2024) studied the Daily maximum 8-hour average (MDA-8) ozone changes and observed that cities such as Visakhapatnam and Tirupati reported zero days of MDA-8 ozone surpassing 100 ppb post the implementation of NCAP in 2022 when compared to that of 2018, the base year, during which Visakhapatnam and Tirupati experienced about 60 and 10 such days, respectively. Nevertheless, some cities in the Indo-Gangetic Plains (IGP) of India, for instance, Agra, Singrauli, Ghaziabad, with decreasing aerosol loading and particulate matter pollution (Gopikrishnan and Kuttippurath, 2025), show an increase in the surface ozone levels. This trade-off between particulate matter (PM) and surface ozone was also mentioned in other highly populated regions of the world. For example, Wang et al. (2020) also observed that the opposite changes in surface ozone and $PM_{2.5}$ emerged as an unforeseen consequence of China's Clean Air Action Plan, aimed at reducing air pollution. Following the implementation of the plan, ozone levels increased over the summer in the North China Plain, due to reduced NO_x emissions and steady or rising VOC emissions, alongside significant decreases in $PM_{2.5}$ concentrations. This indicates that addressing ozone pollution requires deeper knowledge than broadly categorising it as NO_x-limited or VOC-limited, as the influence of PM and aerosols is significant (Zhao et al., 2023). Nevertheless, this variability in PM can also arise substantially due to changes in meteorology (Ivatt et al., 2022). Therefore, future air quality management systems worldwide must include the intricate relationship between ozone, particulate matter, precursor emissions and the regionally prevailing meteorology to effectively reduce both pollutants simultaneously.

Rural pollution is also a critical, yet often overlooked aspect of air quality management, especially in a country like India, where a significant portion of the population resides in rural areas (Pathak and Kuttippurath, 2022; 2024). Rural regions are not immune to air pollution; they face unique challenges such as solid fuel combustion for cooking, agricultural residue burning and increasing vehicular emissions due to expanding road networks (Bhuvaneshwari et al., 2019; Chanana et al., 2023). These activities contribute to elevated levels of PM and ozone precursors, which can drift into urban areas, exacerbating pollution in cities through regional transport mechanisms. Furthermore, rural air pollution has profound implications for public health, as rural populations often lack access to healthcare infrastructure to address respiratory and cardiovascular diseases caused by poor air

quality (Coker and Kizito, 2018; Manisalidis et al., 2020). It also impacts agricultural productivity, with rising ozone levels reducing crop yields, thereby threatening food security in agrarian economies like India (Pandya et al., 2022; Anagha et al., 2023). Addressing rural pollution is essential for achieving holistic improvements in air quality and ensuring equitable environmental health benefits across urban and rural populations.

Studies on the impact of aerosols on near-surface ozone formation have predominantly focused on the significance of Aerosol Optical Depth (AOD) extinction in photochemical processes that generate ozone (Bian et al., 2007; Kim et al., 2013; Wang et al., 2019). AOD quantifies the degree to which aerosols scatter and absorb sunlight, hence influencing the quantity of solar radiation that reaches the Earth's surface. This subsequently affects the photochemical mechanisms that facilitate ozone synthesis in the lower atmosphere. Nevertheless, in areas with high aerosol concentrations, the reduction of surface ozone is not only governed by AOD extinction, but also the aerosol surface area by offering reactive sites for chemical reactions with molecules such as HO_2 (Macintyre and Evans, 2011; Song et al., 2021). The interaction between aerosols and these species leads to the elimination of ozone precursors, including OH radicals, which are vital for ozone production.

In this study, we aim to evaluate the impact of PM_{10} and aerosol surface area on surface ozone pollution in India. Since several studies are available on the air pollution concentrated in the urban regions of India, our analysis therefore explores the ozone formation regimes across entire India, using a high-resolution GEOS-Chem Chemical Transport Model. This allows us to examine the impact of regional and larger scale dynamics of ozone production, which are often influenced by agricultural practices, biomass burning and long-range pollutant transport. By simulating two distinct years—2018 (a high PM_{10} year and low rainfall year) and 2022 (a low PM_{10} year and normal rainfall year) with and without fixed meteorology for the two years—and incorporating/excluding the reactive absorption of HO_2 onto aerosols (via the γHO_2 parameter), we aim to understand how reductions in PM_{10} levels influence aerosol surface area and the secondary ozone chemistry (**Figures S1 and S2**). Furthermore, we categorize ozone generation regimes into NO_x-limited, VOC-limited and Aerosol Inhibited Regime (AIR) regions based on the dominant termination reactions in surface ozone formation for each model grid (Ivatt et al., 2022). Additionally, by scaling down NO_x emissions by 25 and 50%, we assess the efficacy of national and local emission control measures in mitigating NO_x emissions and their subsequent impact on surface ozone levels. This approach provides important insights into the chemistry between PM, precursor emissions and surface ozone across diverse geographical regions in India, highlighting the need for integrated air quality management strategies beyond urban boundaries.

2. Data and Methods

2.1 Region of Study

India can be delineated into six regions based on topographical characteristics, demographic factors, and pollution levels: Peninsular India (PI), Northwest (NW), Northeast (NE), Central India (CI), Indo-Gangetic Plain (IGP), and Hilly Regions (HR), as shown in **Figure 1**. Peninsular India, which encompasses Kerala, Tamil Nadu, Karnataka, Goa, Andhra Pradesh, and Telangana, has three of the ten most populous states—Andhra Pradesh, Tamil Nadu, and Karnataka—and features substantial forest cover in the Western Ghats. Sources of pollution in this region are automobile emissions, industrial operations and biomass combustion, especially in urban areas like

Bengaluru and Chennai. Central India, comprising Maharashtra, Madhya Pradesh, Chhattisgarh, Jharkhand and Odisha, is marked by low population density yet is linked to thermal power plants, coal mines and steel factories. Cities like Mumbai and Pune have higher pollution levels attributable to industrialisation and trash incineration. Northwest India includes Rajasthan and Gujarat, characterised by dry landscapes like the Thar Desert; pollution is attributed to dust from unpaved roads and construction activity, along with industrial emissions from sectors such as textiles. Northeast India comprises Tripura, Mizoram, Manipur, Nagaland, Meghalaya and Assam; despite its low population density and extensive vegetation, this region is affected by automobile pollution and slash-and-burn agriculture methods. The Indo-Gangetic Plain encompasses West Bengal, Bihar, Uttar Pradesh, Haryana and Punjab; it is characterised by a high population density exceeding 1000 individuals per square kilometre and has substantial pollution resulting from heavy traffic, industrial effluents and extensive crop residue burning during harvest periods. The Hilly Regions encompass Jammu and Kashmir, Himachal Pradesh, Uttarakhand, Sikkim and Arunachal Pradesh. These areas are less industrialised and ecologically sensitive, with economies dependent on agriculture and forestry. They experience localised pollution from vehicular emissions and biomass combustion, which is intensified by winter temperature inversions that confine pollutants near the surface (Kuttippurath et al., 2020; Gopikrishnan et al., 2022).

2.2 GEOS-Chem

GEOS-Chem is an extensive model developed for modelling complex oxidant-aerosol chemistry in the troposphere and stratosphere (Zhang et al., 2011; Kim et al., 2015). We have used GEOS-Chem version 14.4.3 in this study (https://doi.org/10.5281/zenodo.13314490). The model complies with the most recent JPL/IUPAC guidelines for chemical mechanisms, with substantial modifications that improve the depiction of diverse chemical processes, including those related to isoprene, aromatics and nitrates (Bates et al., 2024). Recent advancements have enhanced the treatment of complex chemical reactions, including methanol synthesis and mercury redox chemistry, facilitating more precise atmospheric forecasts (Horowitz et al., 2017; Guil-López et al., 2019). Additionally, the model incorporates the reactive absorption of NO_x by aerosols and computes aerosol hygroscopicity, which is essential for comprehending aerosol-cloud interactions. GEOS-Chem offers a comprehensive framework for investigating atmospheric chemistry and its effects on air quality and climate change, accommodating various chemical species and reactions, including halogens and hydroxymethanesulfonate. This model provides thorough understanding into ozone generation mechanisms and pollutant interactions, serving as an essential resource for addressing air quality challenges and comprehending the wider implications of atmospheric dynamics.

GEOS-Chem has been rigorously validated by researchers globally. For instance, Travis and Jacob, (2016) showed that, despite the successful simulation of ozone and its precursors in the SEAC4RS aircraft data below 1 km of altitude, MDA8 surface ozone was biased high in the model by +6 μg/m³ on average. David et al. (2019) used the GEOS-Chem transport model in India and observed that the model reasonably simulated the tropospheric O_3 abundances and vertical profiles, with a mean bias of 1–3 DU compared to observations for the period 2000–2015. Christiansen et al. (2022) found that the GEOS-Chem model, when validated against ozonesonde, aircraft, and satellite observations globally, showed reasonable agreement with a mean bias of 1–3 DU for the period from 1990 to 2017. Mao et al. (2024) reported that the GEOS-Chem model, validated against MDA8 O_3 concentration

observations in central and eastern China from May to July 2017, showed a strong correlation of 0.77 (95% confidence level). In Nanjing, the simulated MDA8 O_3 concentrations converged with the observed trend, with a correlation coefficient of 0.65, a normalised mean bias (NMB) of 5%, and a normalised mean error (NME) of 21%. Karambelas et al. (2022) used the GEOS-Chem model to simulate $PM_{2.5}$ concentrations during high PM episodes in the fall of 2015 and 2017, finding that the model underestimated observed concentrations by 28%, with an average observed $PM_{2.5}$ concentration of 142 $\mu g/m^3$ compared to 125 $\mu g/m^3$ from the model. Pai et al. (2022) validated the GEOS-Chem simulation against speciated airborne aerosol measurements over India and reported significantly reduced normalized mean biases: NMBModified = 0.19 compared to NMBBase = 0.61 overall—with nitrate improving from 1.64 to 0.08 and ammonium from 0.90 to 0.49. Despite this underestimation, the model demonstrated strong spatial correlations with observed concentrations ($r^2 = 0.67$), accurately capturing the spatial distribution of $PM_{2.5}$ across India. David and Ravishankara (2019) used the GEOS-Chem model to estimate boundary layer ozone (BLO_3) contributions across eight regions of the Indian subcontinent, finding that BLO_3 in northern India, Pakistan, and Sri Lanka is largely (about 65–70%) influenced by regions outside the subcontinent. They also highlighted the growing importance of central India in contributing to ozone pollution, with regional meteorology playing a key role in the redistribution of BLO_3 and its precursors including Chlorine (Cl).

In this study, GEOS-Chem is simulated in a 2.0ºx2.5º latitude by longitude grid resolution globally for the boundary conditions for the years 2018 and 2022. One year spin up simulations are used to generate the model restart files and the boundary conditions. The nested model has a grid resolution of 0.25ºx0.3125º latitude by longitude and a spin up period of 1 month. We use the data from the lowest level of the ETA coordinate system from GEOS-Chem model simulations to analyse the correlation between modelled and observed PM_{10} and ozone data. The model is driven by the GEOS–FP assimilated meteorological data provided by the Goddard Earth Observing System (GEOS) of the Earth Modelling and Assimilation Office (GMAO) and with a temporal resolution of 1 hour (Lucchesi, 2013). Emissions in the GEOS-Chem model are handled using the Harvard–NASA Emission Component (HEMCO; Keller et al., 2014). Anthropogenic emissions are derived from the Community Emissions Data System (CEDS), which provides global coverage at a native resolution of 0.1° × 0.1°, with data aggregated to the model resolution (Hoesly et al., 2018). Sea salt emissions are calculated offline following the approach of Zhu et al. (2019), while dust emissions are calculated offline following the method of Ginoux et al. (2010). Emissions of biogenic origin are simulated using the Model of Emissions of Gases and Aerosols from Nature (MEGAN), which provides global emissions at 0.01° latitude × 0.01° longitude resolution (Guenther et al., 2012) and Soil NOx emissions follow the approach outlined by Hudman et al. (2012). Biomass burning emissions are sourced from the Global Fire Emissions Database version 4 (GFED4), which provides a global coverage at 0.25° latitude × 0.25° longitude (Giglio et al., 2013).

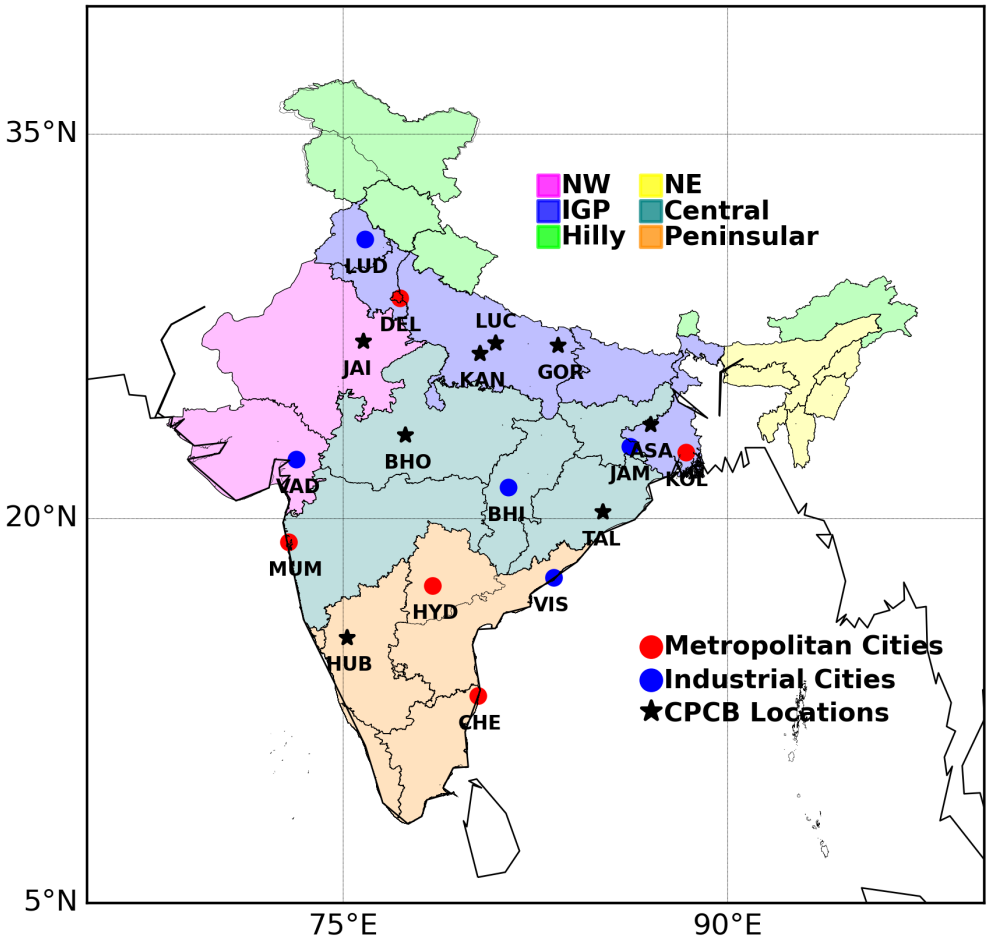

Figure 1: The region of study. The regions considered are also shown in the respective colours. Here, NW is Northwest, NE is Northeast India and IGP is Indo Gangetic Plain. The star marks indicate the respective ground-based stations. The red and blue dots indicate the metropolitan and Industrial cities in India. The abbreviations represent the first three letters of each city considered (e.g. DEL is Delhi), and their full names are given in Figure S3.

GEOS-Chem uses a set of chemical mechanisms implemented with the Kinetic PreProcessor (KPP) (Damian et al., 2002). The standard chemical mechanism in GEOS-Chem has undergone continuous development since the original tropospheric gas-phase scheme of Bey et al. (2001), with subsequent extensions to include aerosol chemistry (Park, 2004), stratospheric chemistry (Eastham et al., 2014), and a detailed tropospheric–stratospheric halogen chemistry module (Wang et al., 2019), which include 299 chemical species (Fritz et al., 2022). Sulfate–nitrate–ammonium aerosols are simulated with a bulk thermodynamic approach (Park, 2004), where gas–particle partitioning is calculated using ISORROPIA II (Fountoukis and Nenes, 2007). Sea salt is represented with two modes distinguishing fine and coarse particles (Jaeglé et al., 2011), while mineral dust is described using four particle size bins (Fairlie et al., 2007). Furthermore, the simple SOA scheme is employed for secondary organic aerosols, based on reversible partitioning of semivolatile products of VOC oxidation (Pye et al., 2010). Furthermore, in GEOS-Chem, PM_{10} is diagnosed as the sum of $PM_{2.5}$ plus size-resolved dust (70% of DST2, all of DST3, 90% of DST4) and coarse sea-salt (SALC scaled by the hygroscopic growth factor, e.g., 1.86 at 35–50% RH), with the final values archived at standard temperature and pressure (STP) using the ideal gas law (GEOS-Chem Support Team, 2023).

Furthermore, we use ground-based measurements from Central Pollution Control Board (CPCB) monitoring sites situated in different regions of India, as shown in **Figure 1** and supplementary **Figure S3**, reflecting a wide array of meteorological conditions. The CPCB monitors ambient ozone using UV photometric methods (based on the absorption of UV light by ozone at 254 nm), chemiluminescence (where ozone reacts with a reagent to produce light that is quantified), and chemical methods (colorimetric reactions providing concentration estimates). PM_{10} is measured using gravimetric analysis (filter-based mass determination after sampling), Tapered Element Oscillating Microbalance or TEOM (continuous real-time mass measurement through frequency change of a vibrating element), and beta attenuation techniques (attenuation of beta radiation as it passes through particle-laden filters to infer mass concentration) and these data are available at a resolution of 1 hour (NAAQS, 2013).

The altitude of the lowest model level may not consistently align with the actual altitude of ground-based monitoring locations, thereby causing inconsistencies between modelled and observed data. Therefore, we calculate the correlation coefficient for the time series of ozone and PM_{10} values at each station to evaluate the strength of the association between these variables, as shown in **Figure S3.** The correlation coefficient between modelled and observed values of PM_{10} and ozone is above 0.6 for most of the stations, except in Jaipur in the northwest, where the correlations are 0.5 and 0.4 for PM_{10} and ozone, respectively. Although these moderate to strong correlations suggest a satisfactory alignment between the model and the facts, certain systematic differences remain. The GEOS-Chem model generally underestimates PM_{10} concentration, possibly attributable to its 0.25^{o}x0.3125^{o} resolution, which fails to account for fine-scale local variations, including point sources of pollution. In contrast, the model often overestimates surface ozone concentrations for most of the stations considered here. Despite the model's higher bias caused by uncertainties in emissions of anthropogenic and biogenic precursors, uncertainties in ozone sinks such as dry deposition, and the coarse resolution of the model limits its ability to capture ozone titration and other localised chemical processes (Westervelt et al., 2019). Our analysis focuses on the differences between simulations for 2018 and 2022, with model performance evaluated using ground-based CPCB observations of surface ozone and PM_{10} (**Figure 2, Figure S4 and Figure S5**). GEOS Chem broadly captures regional patterns of annually averaged PM_{10} and ozone, but ground-based stations show higher PM_{10} in NW and IGP (140–160 $\mu g/m^3$ vs. model 120–140 $\mu g/m^3$, which is about 15–20% low bias) and lower values in CI and PI (about 10–15% high bias). For ozone, the model underestimates HR and IGP peaks by about 10–15% (observed >150 $\mu g/m^3$) while overestimating coastal PI levels by about 10–20% (observed 70–90 $\mu g/m^3$). The model reproduces the temporal patterns reasonably well, with annually averaged differences between modelled and observed values remaining within 10–20% across most stations. Despite a few regionally specific biases (higher relative differences in PM_{10} in cities like Talcher, Noida, Jodhpur during the monsoon season), the consistent performance across two meteorologically different years lends confidence to the overall robustness of the high-resolution GEOS-Chem simulations for India.

2.3 Methods

The aerosol uptake coefficient, which quantifies the efficacy of particles in absorbing reactive gases, substantially impacts surface ozone concentrations (Jacob, 2000). In areas with elevated aerosol concentrations, aerosols possessing a high uptake coefficient can more efficiently eliminate ozone precursors, including HO_2 and other reactive radicals, from the atmosphere (Li et al., 2018). These aerosols interact with atmospheric chemical species,

reducing the levels of OH and HO_2 radicals, which are essential for ozone synthesis. The aerosol uptake coefficient of HO_2 (γHO_2), however, is affected by several factors, including the physical and chemical characteristics of the aerosol particles, such as size, composition and moisture content (George and Abbatt, 2010). These parameters show the efficacy of aerosol interactions with atmospheric radicals, thereby affecting ozone production.

Termination rates of chain reactions were determined using archived species concentrations and physical parameters such as temperature, pressure and humidity, in addition to aerosol properties, as in Ivatt et al. (2022). Although we do not classify radical product generation in peroxyl-radical self-reactions as termination stages, we regard non-radical products as ongoing termination processes. The heterogeneous loss rate of HO_2 was assessed by evaluating the radius and surface area of different aerosol forms from the archived model outputs. For our simulations, we employed a default HO_2 reactive uptake coefficient (γHO_2) of 0.2. Laboratory studies of pure synthetic aerosols indicate lower uptake coefficients ($\gamma HO_2 < 0.2$), whereas real-world aerosol studies reveal values between 0.08 to 0.40, implying that elements such as transition metals may increase aerosol uptake (Kolb et al., 2010; Christian et al., 2018). We have also simulated the model with γHO_2 to be zero to evaluate its impact on ozone formation mechanism. While we presumed H_2O to be the exclusive product of HO_2 absorption, our results remain valid when H_2O_2 is considered. Employing a singular γHO_2 value likely oversimplifies the variability, as existing models fail to account for its temporal oscillations (Stavrakou et al., 2013; Sheehy et al., 2010).

The heterogeneous radical loss rate of HO_2 is determined by iterating through the radius and surface area of various aerosol types, which includes sulfate–nitrate–ammonium thermodynamics, secondary organic aerosol, dust, sea salt, black carbon, and primary organic carbon (Ivatt et al., 2022). These factors, along with temperature and air density, are used to calculate the first-order loss rate of HO_2. Furthermore, emissions and photochemical reactions are strongly affected by seasonal variations in India. The seasons are defined as Winter (December-January-February; DJF), Pre-monsoon (March-April-May; MAM), Monsoon (June-July August-September; JJAS) and Post-monsoon (October-November; ON).

3. Results

3.1 Distribution of Surface Ozone and PM for the years 2018 and 2022

3.1.1 Annual Distribution

Figure 2 shows the annual average PM_{10} and ozone in India for the years 2018 and 2022. The highest PM_{10} concentrations (130–150 μg/m³) occur in the NW dry regions due to dust mobilisation from the Thar Desert (Santra et al., 2018; Kashyap et al., 2024), consistent with studies showing dry and semi-arid areas as key mineral dust sources (Maji and Sonwani, 2022). Ground-based observations here often exceed 160 μg/m³, indicating that the model underestimates by about 10–20%. IGP also shows higher PM_{10} (120–140 μg/m³) from industrial, vehicular and agricultural emissions including biomass and crop-residue burning (Devi et al., 2020; Hassan et al., 2023). Station data shows average concentrations of about 140–160 μg/m³, indicating that model is biased low by about 15%. Despite higher emissions, greater humidity and rainfall promote wet deposition and particle scavenging, lowering levels relative to NW (Sen et al., 2017; Singh et al., 2023). CI records 60–100 μg/m³ with

industrial hotspots up to 130–150 µg/m³ (Lokhande and Khan, 2021; Saini et al., 2023), but observations show about 50–90 µg/m³, suggesting the model slightly overestimates by about 10–15%. NE shows lower levels (40–70 µg/m³) due to sparse population and vegetation sinks (Guttikunda and Nishadh, 2022; Kumari et al., 2025).

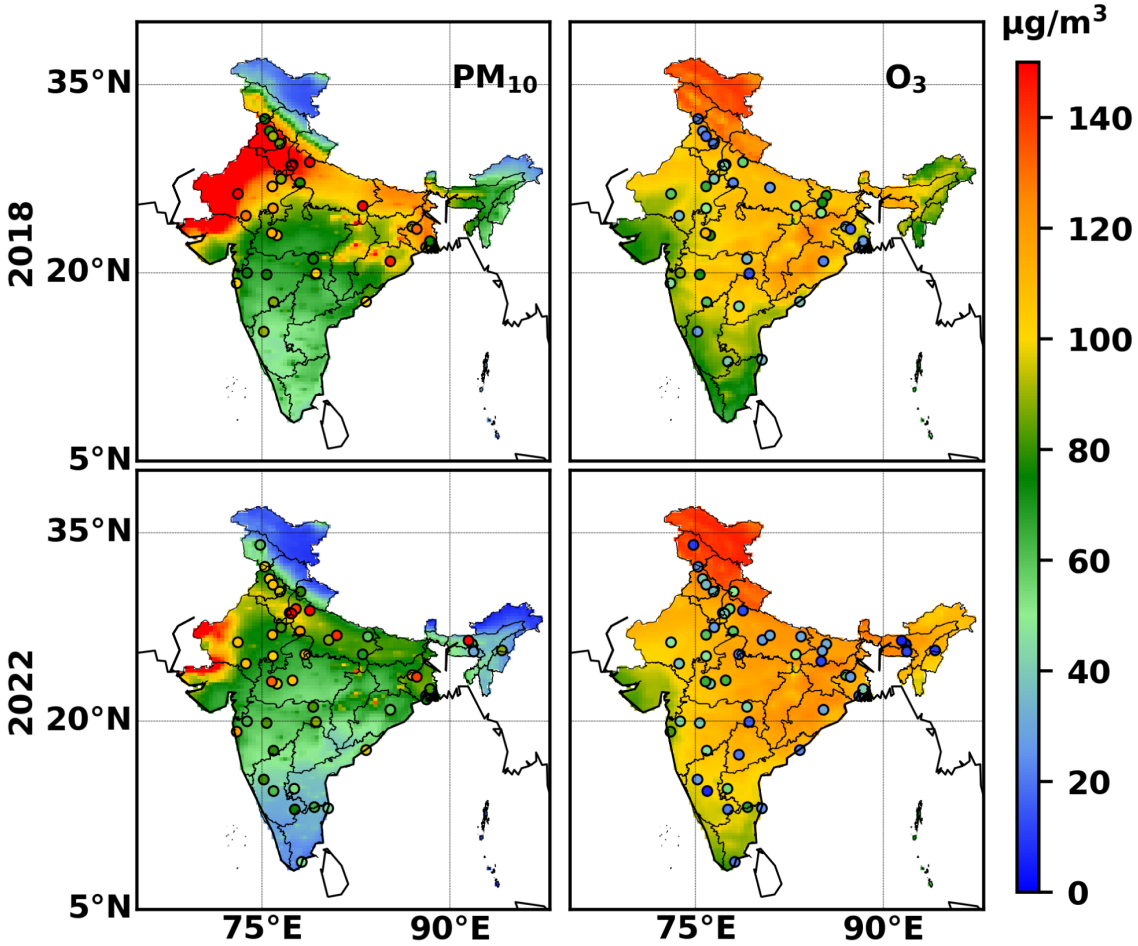

Figure 2: Annual average distribution of PM_{10} and ozone for the years (Top) 2018 and (Bottom) 2022 from GEOS-Chem simulations. The dots show the annually averaged mean values of PM_{10} and ozone at the respective ground-based CPCB stations for the years 2018 and 2022.

Surface ozone peaks in the HR (120–140 µg/m³) due to high stratospheric-to-troposphere transport, Ground-based data here often reach 150–160 µg/m³, showing that model underpredicts by about 15%. (Phanikumar et al., 2017; Wang et al., 2024). High values also occur in IGP and eastern CI (100–120 µg/m³) driven by secondary photochemistry from NOx and VOCs (Payra et al., 2022; Sinha and Sinha, 2019; Mahilang et al., 2021; Kuttippurath et al., 2022) under stagnant conditions (Gopikrishnan and Kuttippurath, 2024). Observations in these regions are typically 110–130 µg/m³, reflecting a model underestimation of about 10–15%. PI shows the lowest ozone (80–100 µg/m³) due to coastal ventilation, humidity, precipitation and oceanic loss, with observed levels closer to 70–90 µg/m³, showing that the model overestimates by about 10–20% (Li et al., 2019; Lakshmi et al., 2024; Galbally and Roy, 1980; Lavanyaa et al., 2023; Nilaya et al., 2024). A detailed discussion of seasonal changes in surface ozone is provided in the supplementary material, **section 1.1**.

Seasonally, PM_{10} is highest in IGP during winter and post-monsoon (100–140 μg/m³) under stable, inversion conditions and intensified biomass and crop-residue burning (Mhawish et al., 2020; Paulot et al., 2022; Jayachandran and Rao, 2024; Payra et al., 2022; Mogno et al., 2021). The NW records its peak during the monsoon from dust storms (Yadav et al., 2022; Yu et al., 2023), while pre-monsoon sees widespread elevated PM_{10} (60–100 μg/m³) with NW reaching 140–160 μg/m³ due to dust, traffic, industrial and construction sources (Patil et al., 2013; Garg and Gupta, 2020). These high levels pose severe health risks, particularly for vulnerable groups (Adhikary et al., 2024; Pathak et al., 2024; Gopikrishnan and Kuttippurath, 2025). Ozone peaks in pre-monsoon, especially over CI, IGP and NE, where it exceeds 140–160 μg/m³, driven by strong solar radiation and abundant precursors (Kutal et al., 2022; Sinha et al., 2014). Winter ozone is also high in CI (100–120 μg/m³), followed by IGP and NE (80–100 μg/m³) under stagnant meteorology and local emissions (David and Nair, 2011; Gao et al., 2020). In contrast, monsoon levels are lowest, with the west coast at 60–80 μg/m³, NW at 80–100 μg/m³ and NE and IGP at 120–140 μg/m³, owing to cloud cover, precipitation and circulation that suppress ozone production and enhance removal (Lal et al., 2014; Lu et al., 2018). Post-monsoon levels are moderate (100–120 μg/m³) across CI, NW and IGP, with PI and NE slightly lower (60–90 μg/m³) (Lu et al., 2018). A detailed discussion of seasonal changes in surface ozone is provided in the supplementary material, **section 1.2**.

3.1.3 Comparison of PM_{10} and Ozone levels

The relationship between PM_{10} and ozone is often inverse, attributable to their distinct formation mechanisms and atmospheric interactions, but varies substantially depending on meteorological conditions and precursor availability (Jia et al., 2017). Higher PM levels, frequent during winter in areas such as IGP, often correlate with lower ozone concentrations (Song et al., 2022). PM disperses and absorbs sunlight, reducing the solar radiation essential for photochemical ozone formation, which depends on NO_x and VOCs concentration in the presence of intense sunlight. Black carbon (BC), a constituent of PM from combustion, can directly scavenge ozone by acting as a deposition surface (Gao et al., 2018). However, this direct BC–ozone scavenging pathway is not explicitly represented in most chemical transport models (Koch et al., 2009), but its overall contribution is considered modest compared to dominant photochemical production and deposition processes, it may still have localised importance in high-BC environments such as South Asia (Kumar et al., 2015). Furthermore, stable atmospheric conditions including temperature inversions that confine PM at the surface also impede vertical mixing, limiting ozone transport from the upper atmosphere, hence facilitating the accumulation of ozone near the surface (Gopikrishnan and Kuttippurath, 2025). In such cases, the co-accumulation of PM and ozone near the surface does not imply a simple inverse relationship, as aerosol–radiation interactions can further suppress the planetary boundary layer (PBL) height (Li et al., 2017; Zou et al., 2017), thereby enhancing pollutant trapping. Under suppressed PBL conditions and high NOx emissions, ozone titration can also occur, leading to additional complexity in the surface ozone response (Lin et al., 2008; Li et al., 2024). Conversely, cleaner environments with reduced PM concentrations enhance ozone generation due to the lack of light scattering and scavenging, which fosters photochemical activity (Rathore et al., 2023; Sicard et al., 2023).

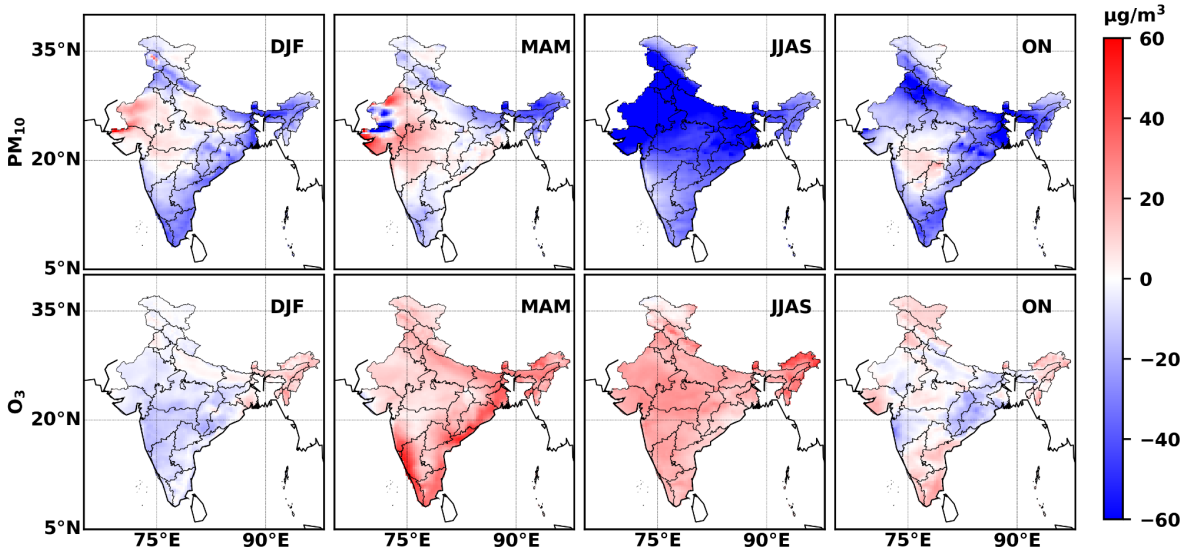

Figure 3: The difference in (Top) PM_{10} and (Bottom) Ozone in 2022 when compared to that of 2018.

Figure 3 shows the change in PM_{10} and ozone in India for the year 2022 when compared to that of 2018. In the monsoon and post-monsoon seasons, PM concentrations drop by 40–60 µg/m³ in the NW, IGP and eastern CI, while reductions of 10–30 µg/m³ occur in other regions, due to changes in the spatial distribution of precipitation as shown in **Figures S6 and S7** (Singh et al., 2023). **Figure S8** presents the changes in aerosol surface area between 2018 and 2022, whereas **Figure S9** illustrates the contributions from different aerosol sources in these two years. The reduction in PM facilitates increased solar radiation penetration, hence promoting photochemical ozone production, resulting in a substantial rise in ozone concentrations (20–30 µg/m³ in most of India during monsoon and 20–30 µg/m³ in PI and western CI during post-monsoon. The decrease in PM_{10} reduces the surface area accessible for heterogeneous processes that might otherwise reduce ozone levels (Gopikrishnan et al., 2025). Conversely, in pre-monsoon and winter seasons, PM concentrations increase by 10–30 µg/m³ regionally, particularly in NW and central IGP, inhibiting ozone formation due to reduced solar radiation and enhanced heterogeneous chemistry that depletes reactive species such as HO_2 (Wang et al., 2024). The stagnant meteorological conditions associated with winter, including temperature inversions, elevated humidity, and minimal wind speeds, intensify PM buildup, particularly in IGP, resulting in further reductions in ozone levels (Gopikrishnan and Kuttippurath, 2024). Nonetheless, geographical disparities remain, exemplified by a 20 µg/m³ reduction in PM in the Upper Northeast of IGP during pre-monsoon, which causes a 20–30 µg/m³ rise in ozone levels, and a 10–20 µg/m³ decline in PM near the west coast, resulting in a 40–60 µg/m³ increase in ozone. In winter, ozone variations are negligible (within 10 µg/m³) over much of India; however, a reduction in PM (10–30 µg/m³) in the northeast correlates with a 20–30µg/m³ rise in ozone levels. The seasonal variability is additionally affected by the aerosol-photolysis feedback, wherein PM influences ozone by absorbing important species such as H_xO_y and NO_x, hence reducing surface photolysis rates and inhibiting ozone production (Ivatt et al., 2022; Gopikrishnan et al., 2025).

4. Discussion

4.1 Impact of HO_2 uptake onto aerosol on surface ozone

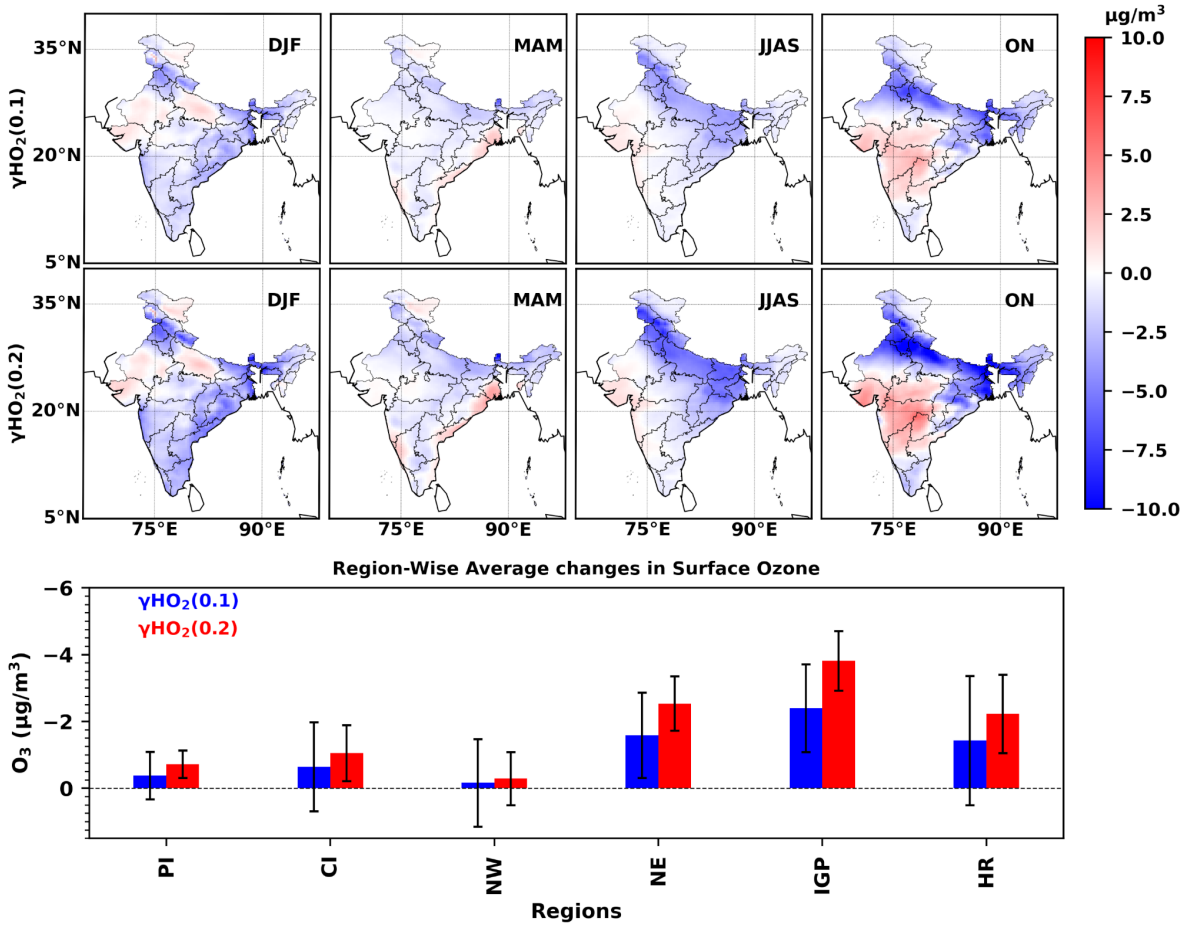

Figure 4: Difference in surface ozone response to aerosol uptake between 2022 and 2018, expressed relative to the no-uptake case ($\gamma HO_2 = 0$). The top panel shows [(O_3 at $\gamma HO_2 = 0.0$ in 2022 – O_3 at $\gamma HO_2 = 0.1$ in 2022) – (O_3 at $\gamma HO_2 = 0.0$ in 2018 – O_3 at $\gamma HO_2 = 0.1$ in 2018)], while the middle panel shows the analogous calculation for $\gamma HO_2 = 0.2$. The bottom panel shows the change in surface ozone averaged for the entire year when $\gamma HO_2 = 0.1$ and $\gamma HO_2 = 0.2$. The bottom panel presents a bar chart of regionally averaged annual surface ozone changes for $\gamma HO_2 = 0.1$ and $\gamma HO_2 = 0.2$, derived from the top and middle panels. Here, negative values indicate stronger ozone suppression in 2018, while positive values indicate stronger suppression in 2022.

The GEOS-Chem model simulations for 2018 and 2022 were performed without and with aerosol uptake of HO_2 to study the impact of γHO_2 on surface ozone concentrations in India in the absence of this mechanism. The results show that the aerosol absorption of HO_2 substantially influences ozone concentrations, as shown in **Figure 4,** especially in areas like the IGP and eastern CI. The increase in ozone concentrations in these regions without aerosols (**Figure S10**), attributed to the absorption of HO_2 by aerosols, varies from 5 to 10 μg/m³, with the most significant changes during winter and post monsoon season. Winter season is defined by higher aerosol surface area, which promotes heterogeneous processes that enhance the removal of HO_2, hence restricting its availability for ozone formation (Dyson et al., 2022). In 2022, aerosol concentrations rose substantially in winter when

compared to 2018, especially in the middle IGP and western CI. This augmentation of aerosol surface area in 2022 inhibited ozone generation by about 5–7.5 μg/m³ in these areas. The most notable changes in ozone concentrations were during post-monsoon, with an increase of about 5–10 μg/m³ when no aerosol absorption is considered, especially in IGP and western CI. In 2022, there was a rise in aerosol surface area in western CI compared to 2018, resulting in an additional suppression of surface ozone. The pre-monsoon season period had similar changes in ozone concentration, with an increase of about 2.5–5 μg/m³, whereas the monsoon period observed minimal variation, with ozone concentration changes between 0 and 5 μg/m³. Thus, the changes in ozone concentrations are directly influenced by aerosol surface area, which amplifies the heterogeneous elimination of HO_2, thereby restricting its availability for ozone synthesis (Anurose et al., 2024). Seasonal fluctuations in aerosol load, influenced by factors like monsoon dynamics, atmospheric transport, and emissions, greatly influence the effects of aerosol-HO_2 interactions on ozone levels. The rise in aerosol concentrations in 2022, especially during winter and post-monsoon, can be attributed to higher anthropogenic activities increasing sulphate, BC and OC, which enhance the suppression of ozone production in these seasons (Austin et al.,2015; Zhang et al, 2023).

In addition to the simulation with a γHO_2 of 0.2, a sensitivity analysis using $\gamma HO_2 = 0.1$ was conducted for the years 2018 and 2022, as shown in **Figure 4** and **Figure S11**, respectively. This lower value was chosen, as previous studies suggest that $\gamma HO_2 = 0.2$ may overestimate heterogeneous uptake, particularly over East Asia, where values closer to 0.1 have been reported under typical ambient conditions (Yang et al., 2023). Given the large uncertainty and variability in γHO_2 arising from factors such as aerosol composition, relative humidity, and particle acidity (Lakey et al., 2024), it is critical to assess the sensitivity of modeled ozone to a range of uptake efficiencies. This uncertainty can lead to substantial differences in simulated ozone, as even a halving of γHO_2 (from 0.2 to 0.1) significantly reduces the magnitude and spatial extent of ozone suppression. The comparison between the two scenarios indicates that the impact on surface ozone concentrations is both spatially and seasonally dependent, with $\gamma HO_2 = 0.2$ yielding a more pronounced and widespread increase when compared to a no aerosol uptake scenario. During the DJF and ON seasons, the increase in ozone is up to 10 μg/m³ across IGP, eastern, and central India, while the $\gamma HO_2 = 0.1$ simulation shows more modest reductions in the range of 5–10 μg/m³ over similar regions. In the MAM and JJAS seasons, the differences in ozone concentrations are comparatively weaker in both scenarios, generally within 0 to 5 μg/m³, although localized reductions persist over northern and eastern parts of India. The interannual differences (2022–2018) shows a consistent spatial pattern, particularly when γHO_2 is 0.1, where negative anomalies of up to 7.5 μg/m³ are observed across northern and central India. Additionally, small positive anomalies (up to 3 μg/m³) are observed in isolated regions such as parts of western Rajasthan, Gujarat and southern peninsular India.

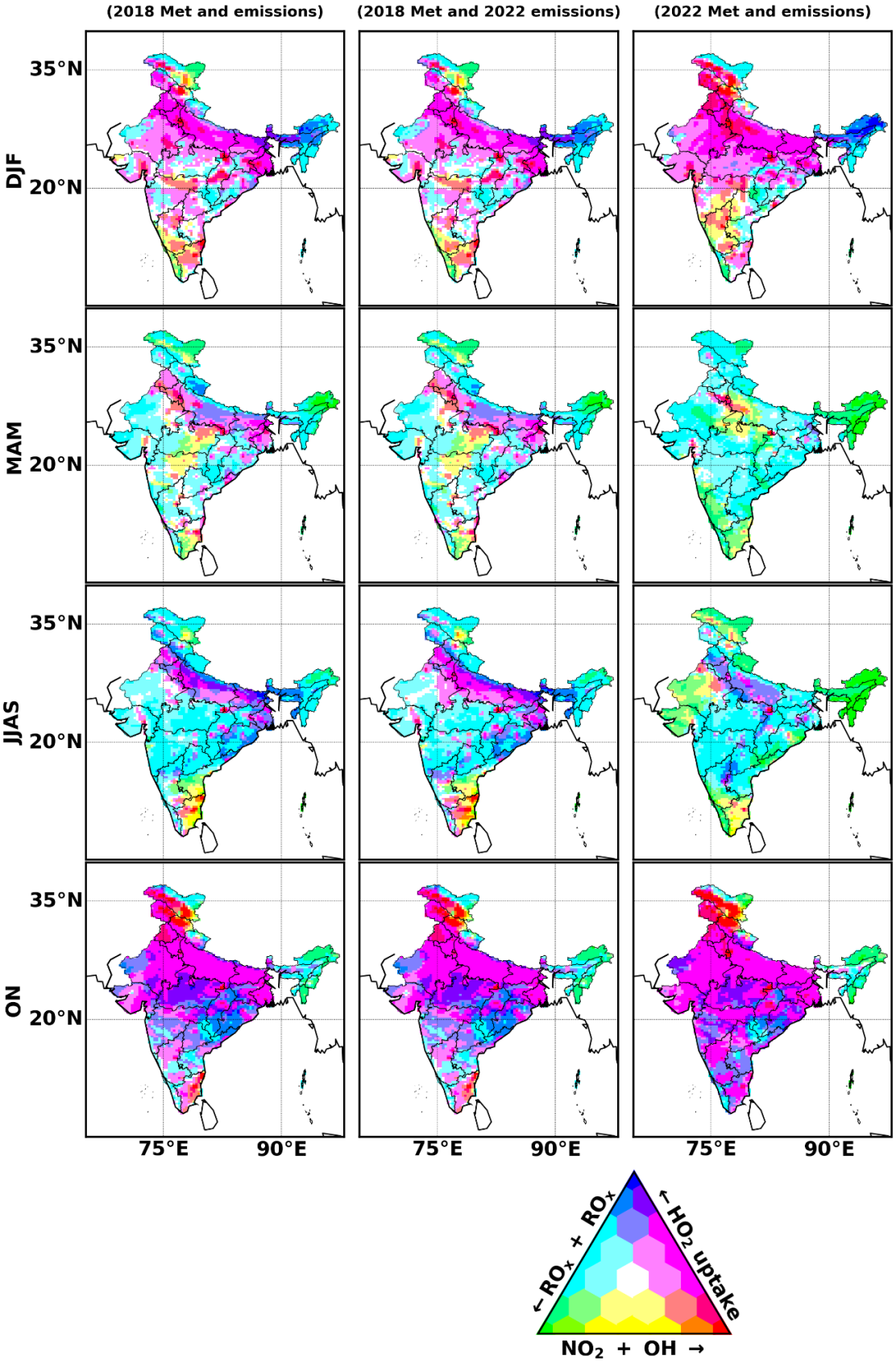

403

404 **Figure 5: Mean fraction of radical termination at the surface that occurs through OH + NO_2 (red), peroxyl-radical self-**
405 **reactions (green) and aerosol uptake of HO_2 (blue) for the year (left) 2018 and (right) 2022.**

4.2 Surface Ozone Formation Regimes

Figure 5 shows the surface distribution of the relative chemical fluxes associated with the termination steps of ozone formation in India for the years 2018 and 2022. During monsoon in 2022, peroxyl-radical self-reactions (green) dominate most of PI, NE and NW arid regions, while in 2018, ozone termination was equally influenced by NO_2+OH reactions and peroxyl-radical self-reactions in PI, whereas NW and NE by HO_2 uptake onto aerosols (blue). When emissions are updated to 2022 levels but meteorology is fixed at 2018 (middle column), the chemical regimes remain almost similar, indicating that meteorology contributes substantially to the changing chemical regimes, as found in the 2022 meteorology and chemistry coupled simulations (third column). The peroxyl-radical self-reactions are more widespread across major cities in India (for e.g., Visakhapatnam, Delhi and Hyderabad), reflecting the reduced availability of NOx as a radical sink. This weakening of NO_2+OH termination is particularly evident outside IGP, where declining NOx emissions shift the balance toward radical–radical termination pathways. Thus, the dominance of peroxyl-radical self-reactions indicates that NO_x emissions in these cities limit ozone formation, promoting pathways where peroxy radicals neutralize ozone, through the VOC limited ozone formation regime (Romer et al., 2018).

During winter, NO_2+OH termination and the uptake of HO_2 on aerosols became prominent over much of India, particularly in IGP. The increased aerosol surface area during this period enhances the uptake of HO_2, thereby inhibiting ozone production (**Figure S8** and **Figure S9)**. The presence of aerosols, often exacerbated by biomass burning and dust transport, amplifies this effect in areas where aerosols are abundant (Ivatt et al., 2022; Singh et al., 2018). Under fixed 2018 meteorology with 2022 emissions, the chemical termination mechanisms remain similar in most regions. Nevertheless, we observe the dominance of HO_2 uptake chemical termination in the PI region in 2022 when model simulations are coupled with the 2022 meteorology and emissions. In post-monsoon, the termination of ozone formation shifts predominantly to HO_2 uptake across many regions, particularly in IGP, CI, and parts of PI. The NE, however, is an exception, where peroxyl-radical self-reactions continue to dominate the termination process. This variation in termination pathways can be attributed to regional differences in aerosol loading and the influence of seasonal emissions, including biomass burning during the post-monsoon season, which contributes to higher aerosol concentrations in IGP and CI. The fixed meteorology simulations show that the spatial extent of chemical termination mechanisms closely resembles the results of the simulations with 2022 emissions and 2018 meteorology in ON.

During the pre-monsoon period in 2022, the southern parts of northern IGP are predominantly influenced by HO_2 uptake, whereas the rest of IGP and much of India find dominant termination by peroxyl-radical self-reactions. The increased aerosol surface area and the presence of fire events, particularly in the dry regions of NW and NE regions, enhance the uptake of HO_2, suppressing ozone formation (Kumari et al., 2025). Fire events and desert dust also contribute to higher aerosol concentrations, reinforcing the impact of heterogeneous reactions on ozone chemistry (Dyson et al., 2023; Dhanurkar et al., 2024). With 2018 and 2022 emissions under 2018 meteorology, the chemical termination in MAM is clearly through peroxyl-radical reactions and NO_2 + OH regimes, except in IGP where HO_2 uptake dominated the chemical termination mechanism, which can be attributed to high fire activity and dust loading (Kuttippurath et al., 2022).

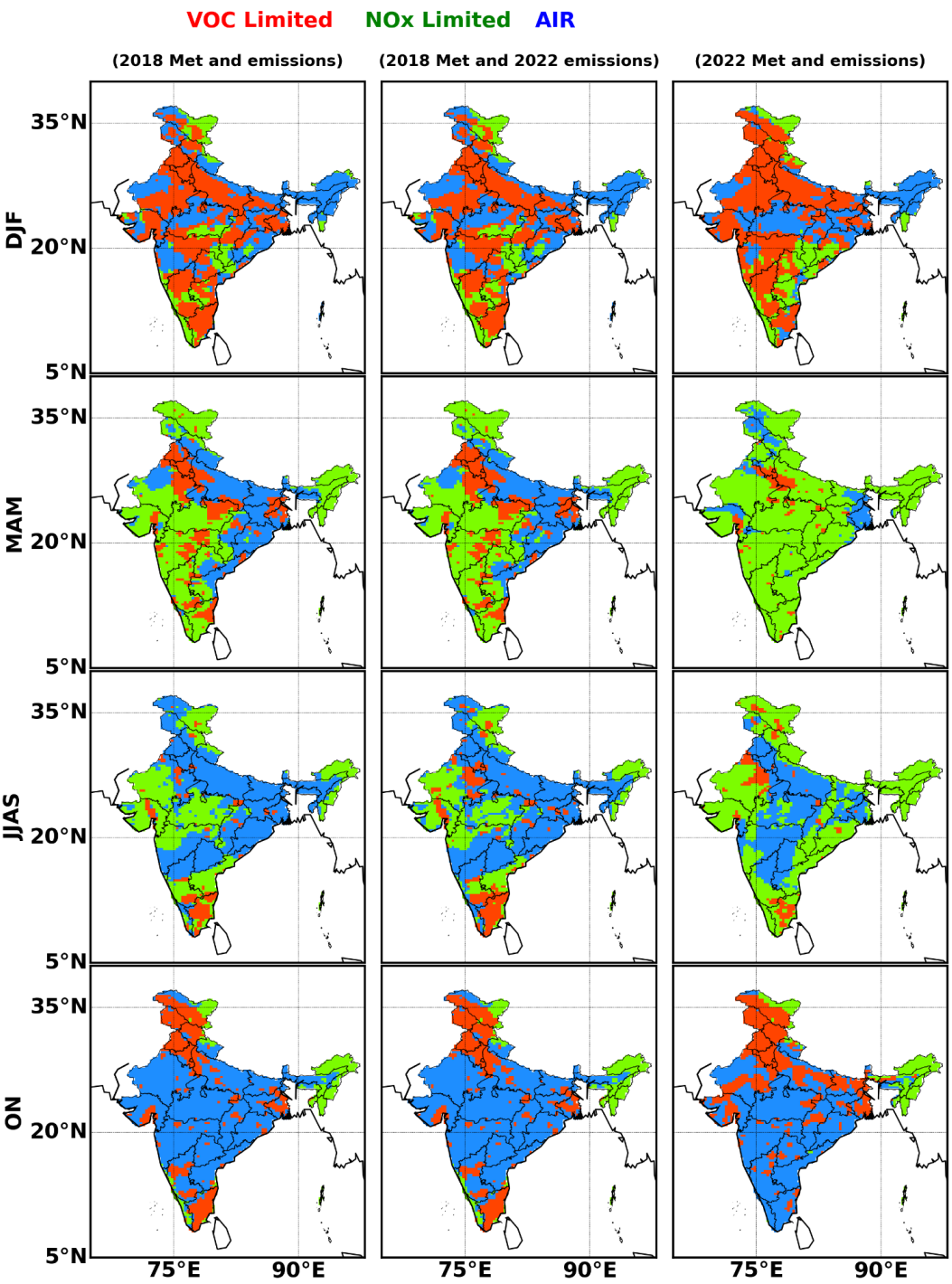

443

444 **Figure 6: The regional distribution of various ozone generation photochemical regimes modelled with γHO2 of 0.2 in**
445 **(left) 2018 and (right) 2022. Here, AIR is Aerosol Inhibited Regions.**

446 Furthermore, **Figure 6** splits the domain based on the local largest termination step. In regions characterized as
447 'NO_x-limited,' the peroxy self-reactions dominate, making reductions in nitrogen oxides (NO_x) the most effective
448 strategy for mitigating ozone pollution; this contrasts with 'VOC limited' regimes, where VOC reductions are
449 more beneficial, with the transition between these regimes dictated by the atmospheric concentrations of NO_x and

VOCs. Aerosol uptake of hydroperoxyl radicals (HO_2) on aerosol surfaces can lead to an 'aerosol inhibited' environment, diminishing ozone formation in areas with elevated aerosol concentrations.

In 2018, much of IGP and CI were in an AIR during summer and monsoon, where the presence of aerosols, particularly in regions with high anthropogenic emissions and biomass burning, suppressed ozone formation by promoting the heterogeneous uptake of HO_2. However, a substantial reduction in aerosol surface area in 2022, shifted some of these regions into a NO_x-limited regime (for e.g. eastern CI, eastern IGP), where the availability of NO_x becomes the limiting factor for ozone formation. This transition to a NO_x-limited regime is associated with a subsequent increase in ozone concentrations in 2022 compared to 2018, as the reduction in aerosols resulted in more ozone to form via the photochemical pathways involving NO_x and VOCs. The decrease in aerosol surface area, coupled with reduced aerosol-induced HO_2 removal, enhanced the ozone production efficiency, leading to higher ozone levels in these regions. Nevertheless, when emissions are updated to 2022 but meteorology is fixed for 2018, large parts of CI, PI, and NE transit out of AIR into NOx-limited regimes. This shows that emission reductions, particularly in NOx, are sufficient to drive regime shifts, but the meteorological changes also play a major role in these regions, with IGP remaining the strongest VOC-limited hotspot among the urban centers.

In contrast, during winter and post-monsoon, there is less to no difference in the dominant regimes between 2022 and 2018. In winter, most of India remains in a VOC-limited regime, where VOCs (such as those from biogenic sources and fossil fuel emissions) limit ozone formation. CI and NE continue to be in AIR during this period, with high aerosol concentrations suppressing ozone production through HO_2 uptake. During post-monsoon, the majority of India remains in AIR, except for northern IGP, which is in a VOC-limited regime, and NE, where the region is predominantly NO_x-limited. The fixed meteorology simulations show that, during the post-monsoon season, the western coast turns out to be in an AIR, whereas this region is NOx-limited in the 2022 meteorology simulations. However, IGP remains strongly VOC-limited due to persistent high NOx emissions and stagnant meteorological conditions, mostly during DJF and partly in ON. The seasonal consistency in winter and post-monsoon suggests that the aerosol levels together with the overall seasonal and regional variations in emissions, meteorology and chemistry play a larger role in initiating the ozone formation regime in these periods. Therefore, while aerosol changes in 2022 had a notable impact on ozone production during monsoon, they had a lesser influence on the seasonal regimes in winter and post-monsoon. This enhanced sensitivity during the monsoon is attributable to elevated humidity and aerosol liquid water content, stronger photochemical radical production, and deeper boundary layer dynamics, which collectively amplify the influence of aerosol uptake on ozone formation relative to winter or post-monsoon.

4.3 Impact of meteorology on surface ozone formation regimes

The interannual comparison shows that surface ozone variability in India is governed primarily by meteorological drivers, with a secondary contribution from emission-induced changes in PM and associated HO_2 uptake. The difference between 2018 and 2022 (**Figure 3**) shows large and spatially coherent ozone anomalies, often exceeding ±20–60 μg m^{-3} across northern and central India. These differences are most pronounced during MAM and JJAS, when enhanced solar radiation, elevated temperatures, and changes in circulation patterns strongly modulate precursor availability and photochemical activity (Rathore et al., 2023). For instance, ozone increases of about 30–40 μg m^{-3} are evident across northern India during JJAS, coinciding with large PM reductions (>40

μg m^{-3}), while the signal is weaker in southern India (about 10–15 μg m^{-3}), reflecting the combined influence of regional circulation and boundary layer dynamics (Gopikrishnan and Kuttippurath, 2024). Such large magnitudes strongly suggest that the direct impact of meteorology on surface ozone pathways, through direct modulation of precursor lifetimes, photolysis rates and vertical mixing also exert dominant influence on ozone variability.

In contrast, the isolated influence of aerosol HO_2 uptake, as represented in the γHO_2 sensitivity simulations (**Figure 4**), yields substantially smaller ozone changes, typically limited to about 5–10 μg/m^3. This is most visible in IGP and eastern coasts of India, where high PM levels enhance HO_2 uptake, thereby suppressing ozone formation under polluted conditions. However, even in these regions, the HO_2 uptake effect is an order of magnitude smaller than the direct meteorological impact (20–40 μg/m^3). The radical termination budget (**Figure 5**) provides mechanistic clarity: across most of India, ozone termination is dominated by $OH+NO_2$ reactions (accounting for about 60–70%), whereas the contribution of HO_2 uptake is rarely about 20–30%, and is substantial only in persistently polluted environments (cities/urban regions). This means that while aerosol uptake of HO_2 can influence local ozone production regimes by shifting the balance between propagation and termination, its influence on interannual ozone variability is minor compared to the large-scale and seasonally varying imprint of meteorology.

However, in future, the relative balance between these pathways is expected to evolve. As PM concentrations decline due to emission controls, the buffering capacity of aerosol HO_2 uptake will weaken, leaving ozone formation increasingly sensitive to direct meteorological perturbations. Under present conditions, the PM–HO_2 uptake pathway contributes only about 10–20% of the ozone variability seen in **Figure 5**. However, in a future low-PM environment, even normal fluctuations in rainfall and atmospheric circulation could lead to disproportionately higher ozone. For example, during dry years with reduced wet scavenging and enhanced precursor accumulation, the absence of strong PM sinks may amplify ozone increases relative to normal or wet years, particularly in NO_x-rich urban regions of northern India. This suggests that while emissions have already reduced the potential for PM-driven radical termination, the dominant role of meteorology in setting ozone levels will likely strengthen, leading to more frequent and intense ozone enhancements during adverse meteorological episodes. Therefore, to counteract the enhanced ozone production expected under declining PM conditions, additional NO_x controls will be essential.

4.4 Impact of the national efforts in reducing NO_x and its effect on surface ozone pollution

National and local efforts to reduce NO_x emissions in India have had a noticeable impact on surface ozone pollution, particularly in urban and industrialized regions (Chen et al., 2021; Misra et al., 2021; Gopikrishnan et al., 2022). NO_x, primarily emitted by vehicular traffic, power plants and industrial processes, plays a critical role in the formation of surface ozone through photochemical reactions. By reducing NO_x emissions, several regions in India have observed a significant decrease in ozone formation. National initiatives such as stricter emission standards for vehicles, the promotion of cleaner fuels, and the adoption of advanced technologies in industrial operations have contributed to the reduction in NO_x emissions (UNESCAP, 2022). These efforts are particularly impactful in regions like IGP, which has been a hotspot for high NO_x concentrations and consequent ozone pollution. Furthermore, policies aimed at reducing vehicular traffic, such as improved public transport systems and the promotion of electric vehicles, have shown promise in lowering NO_x levels and mitigating surface ozone

formation (Saikia, 2025). These measures help disrupt the photochemical cycle that leads to high ozone levels, as lower NO_x concentrations slow down ozone generation. However, the success of these efforts is often offset by increasing emissions from other sectors, such as agriculture, where practices like biomass burning continue to release NO_x (Usmani et al., 2020). Despite these challenges, sustained efforts to reduce NO_x emissions have contributed to a gradual improvement in air quality, particularly in urban centers, leading to a secondary reduction in surface ozone pollution in time. Nevertheless, more stringent emission reductions are required to tackle the increasing ozone problem in India. Therefore, we scaled down the emissions of NO_x in the model simulations to see how this decrease in NO_x would facilitate the ozone generation or destruction in different regions of India. **Figure S12** shows the impact of 25% and 50% NOx emission cuts on aerosol surface area. Eastern India and the IGP region experience the most substantial reduction in aerosol surface area due to NOx reductions, especially during the post-monsoon (ON) and winter (DJF) periods. In the 50% reduction scenario, the decrease in these areas reaches values as low as -4 x 10^{-7} cm^2 cm^{-3}.

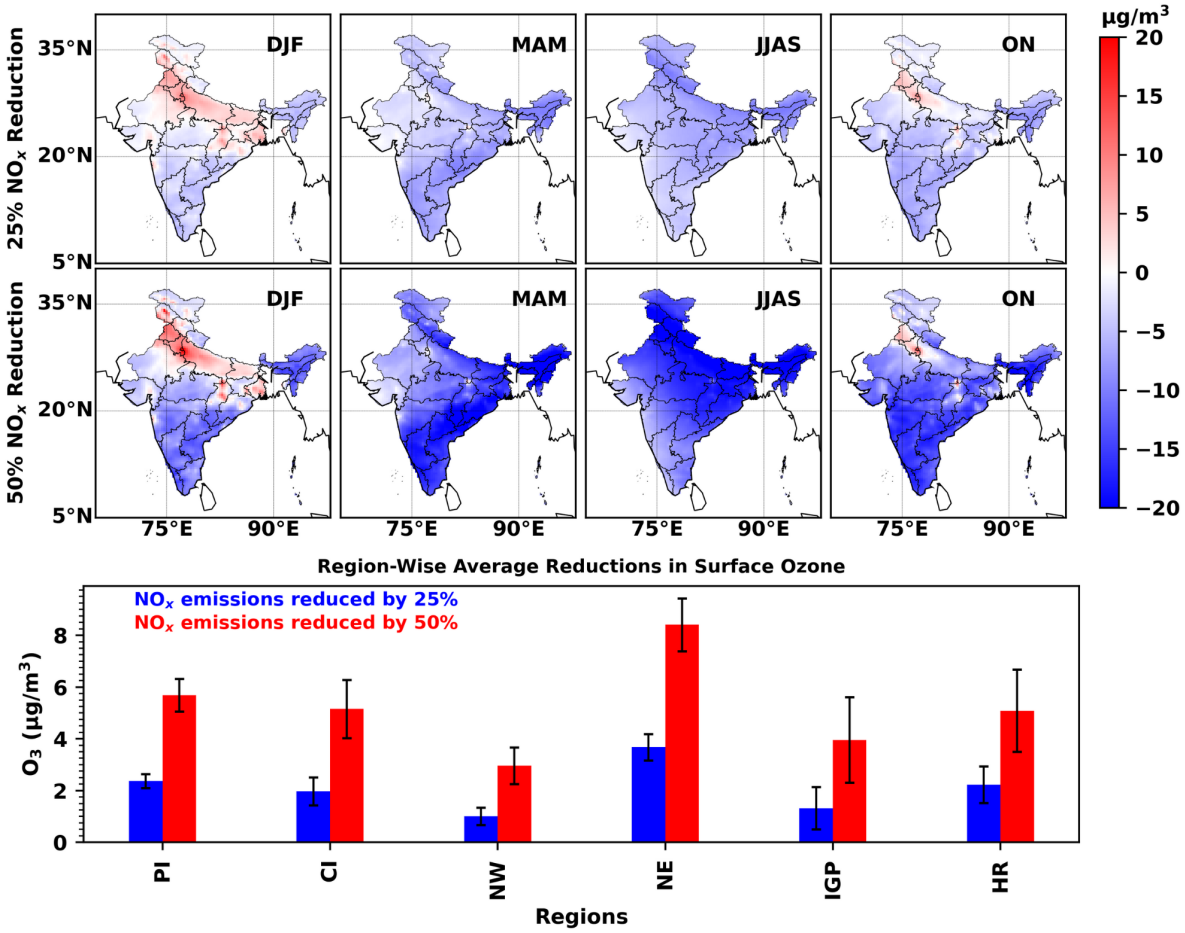

Figure 7: The change in ozone levels when NOx emissions are scaled down by (top) 25% and (middle) 50% when compared to that of base simulation in 2022 with no reduction of emissions. (bottom) Region-wise averaged surface ozone reduction when NOx emissions are scaled down by 25 and 50% for the year 2022. The whiskers represent the standard deviations. Here, PI is Peninsular India, CI is Central India, NW is NorthWest, NE is North East India, IGP is Indo-Gangetic Plains and HR is Hilly Regions.

Figure 7 shows the difference in surface ozone in 2022 with 25% and 50% reduction in NO_x emissions when compared to that of 2022 with no reduction in emissions. A decrease of approximately 5–10 μg/m³ in ozone levels is found with a 25% reduction in NO_x emissions, while a 10–15 μg/m³ decrease occurs with a 50% reduction in NO_x emissions in India. The most substantial reduction occurs during the monsoon season, characterised by a NO_x-limited regime prevalent throughout much of India, succeeded by the post-monsoon and pre-monsoon periods. During winter, particularly in IGP and eastern CI, ozone levels increase, as these regions are limited by VOCs during this period. The increase is about 5–10 μg/m³ with a 25% decrease in NO_x emissions, and about 10–15 μg/m³ with a 50% reduction. Additionally, regional variations in ozone reduction are more pronounced in the 50% decrease scenario, while the 25% reduction shows a more uniform decrease across India (5–10 μg/m³). The reduction of ozone is most noticeable in PI during pre-monsoon and post monsoon (10–15 μg/m³), but, the ozone reduction occurs primarily during monsoon in IGP (10–15 μg/m³), with the smallest levels (5–10 μg/m³) in PI. The seasonal change can be due to decreased NO_x levels in the PI during the monsoon, as rainfall significantly removes precursors in the atmosphere during this season. The findings indicate that roughly 75–80% of the ozone increase attributed to the decrease in PM and aerosols in India could possibly be alleviated through enhanced regulation of NO_x emissions. Also, the findings suggest that winter strategies must focus on reducing VOCs, whereas stricter NO_x control efforts are essential in other seasons to mitigate ozone pollution.

5. Conclusions

This study examines the interactions between PM_{10}, aerosols and surface ozone concentrations in India, focusing on the changes modelled between 2018, a higher PM_{10} year, and 2022, a lower PM_{10} year. The findings highlight that the seasonal and regional variability of PM_{10} and aerosol surface area play a major role in modulating surface ozone formation. During winter and post-monsoon seasons, elevated PM_{10} and aerosols, particularly in IGP and CI, led to higher uptake of HO_2, reducing its availability for ozone production and hence suppressing ozone levels by about 30–40% when compared to the surface ozone levels in 2018 and 2022. However, during monsoon and pre-monsoon seasons, reduced aerosol surface area and PM concentrations enhance photochemical ozone formation, as the decrease in aerosol surface area allows more HO_2 to participate in ozone production. The shift from an aerosol-inhibited regime to a NO_x-limited regime in 2022, due to lower aerosol pollution compared to 2018, resulted in an increase in ozone levels in several regions, especially in the IGP contributing to an increase in its levels by about 20–30 μg/m³. This suggests that the balance between aerosols, NO_x and VOCs dictates ozone formation, with aerosol concentrations continuing to significantly influence ozone levels during these seasons. Nevertheless, local emissions from vehicular traffic, regional transportation, industrial operations, household sources and agricultural residue combustion substantially control PM_{10} and ozone levels, highlighting the necessity for thorough, region-specific emission control measures. Furthermore, scaling down the NOx emissions in the model simulations by 25 and 50% shows a spatial variability in the reduction of surface ozone, with decreases of about 5–10 and 10–15 μg/m³ across India, respectively. Thus, this unintended increase in surface ozone due to the decrease in PM and changing meteorological conditions can be reduced by additional efforts in reducing anthropogenic NO_x emissions. Therefore, this study recommends the need for integrated air quality management strategies that consider both aerosol and precursor emissions, along with regional meteorological patterns, to address ozone pollution in India effectively.

Data availability. GEOS-Chem model is available via https://geos-chem.readthedocs.io/en/stable/ and CPCB data is available via https://app.cpcbccr.com/ccr/

Authorship Contributions. GSG: Writing – review & editing, Writing – original draft, Visualization, Validation, Software, Methodology, Investigation, Formal analysis, Data curation. DMW: Writing – review & editing, Writing – original draft, Supervision, Visualization, Validation, Software, Methodology, Investigation, Conceptualisation. JK: Writing – review & editing, Writing – original draft, Supervision, Visualization, Validation, Methodology, Investigation, Conceptualisation.

Acknowledgements. We thank all the data managers and the scientists who made available those data for this study. GSG acknowledges the Prime Minister's Research Fellowship (PMRF; Grant No: 2402787), Ministry of Education, India, for funding his Doctoral study at IIT KGP and the United States India Education Foundation for his grant through the Fulbright-Kalam Climate fellowship for Doctoral Research (Grant No: 3067/FNDR/2024-2025) at the Lamont-Doherty Earth Observatory and Columbia Climate School, Columbia University, New York. JK and GSG thank the Director, Indian Institute of Technology Kharagpur (IIT Kgp), HoC, CORAL IIT Kgp and the Ministry of Education (MoE) for facilitating the study.

Competing interests. One author (JK) is an editor of ACP. The authors declare there is no other competing interest.

Financial Support. This project was supported by National Science Foundation grant OISE 2020677.

References

Adhikary, M., Mal, P. and Saikia, N.: Exploring the link between particulate matter pollution and acute respiratory infection risk in children using generalized estimating equations analysis: a robust statistical approach. Environmental Health, 23(1), 12. https://doi.org/10.1186/s12940-024-01049-3, 2024

Anagha, K.S., Kuttippurath, J., Sharma, M. and Cuesta, J.: A comprehensive assessment of yield loss in rice due to surface ozone pollution in India during 2005–2020: A great concern for food security. Agricultural Systems, 215, 103849. https://doi.org/10.1016/j.agsy.2023.103849, 2024

Anderson, H.R., Atkinson, R.W., Bremner, S.A., Carrington, J. and Peacock, J.: Quantitative systematic review of short term associations between ambient air pollution (particulate matter, ozone, nitrogen dioxide, sulphur dioxide and carbon monoxide), and mortality and morbidity. Report to Department of Health revised following first review. https://assets.publishing.service.gov.uk/media/5a7507c2e5274a3cb2869199/dh_121202.pdf, 2007

Anurose, T.J., Jayakumar, A., Sandhya, M., Gordon, H., Aryasree, S., Mohandas, S., Bhati, S. and Prasad, V.S.: Unraveling the Mechanism of the Holes in the Blanket of Fog Over the Indo-Gangetic Plains: Are They Driven by Urban Heat Islands or Aerosol?. Geophysical Research Letters, 51(10), e2023GL107252. https://doi.org/10.1029/2023GL107252, 2024

Austin, E., Zanobetti, A., Coull, B., Schwartz, J., Gold, D.R. and Koutrakis, P.: Ozone trends and their relationship to characteristic weather patterns. Journal of exposure science & environmental epidemiology, 25(5), 532–542. https://doi.org/10.1038/jes.2014.45, 2015

Avnery, S., Mauzerall, D.L., Liu, J. and Horowitz, L.W.: Global crop yield reductions due to surface ozone exposure: 2. Year 2030 potential crop production losses and economic damage under two scenarios of O3 pollution. Atmospheric Environment, 45(13), 2297–2309. https://doi.org/10.1016/j.atmosenv.2011.01.002, 2011

Bates, K., Evans, M., Henderson, B. and Jacob, D.: Impacts of updated reaction kinetics on the global GEOS-Chem simulation of atmospheric chemistry. EGUsphere, 2023, 1–18. https://doi.org/10.5194/egusphere-2023-1374, 2023

Bey, I., Jacob, D. J., Yantosca, R. M., Logan, J. A., Field, B. D., Fiore, A. M., Li, Q., Liu, H. Y., Mickley, L. J., and Schultz, M. G.: Global modeling of tropospheric chemistry with assimilated meteorology: Model description and evaluation, J. Geophys. Res., 106, 23073–23095, 2001.

Bhuvaneshwari, S., Hettiarachchi, H. and Meegoda, J.N.: Crop residue burning in India: policy challenges and potential solutions. International journal of environmental research and public health, 16(5), 832. https://doi.org/10.3390/ijerph16050832, 2019

Bian, H., Han, S., Tie, X., Sun, M. and Liu, A.: Evidence of impact of aerosols on surface ozone concentration in Tianjin, China. Atmospheric Environment, 41(22), 4672–4681. https://doi.org/10.1016/j.atmosenv.2007.03.041, 2007

Chanana, I., Sharma, A., Kumar, P., Kumar, L., Kulshreshtha, S., Kumar, S. and Patel, S.K.S.: Combustion and stubble burning: A major concern for the environment and Human Health. Fire, 6(2), 79. https://doi.org/10.3390/fire6020079, 2023

Chen, Y., Beig, G., Archer-Nicholls, S., Drysdale, W., Acton, W.J.F., Lowe, D., Nelson, B., Lee, J., Ran, L., Wang, Y. and Wu, Z.: Avoiding high ozone pollution in Delhi, India. Faraday Discussions, 226, 502–514. https://doi.org/10.1039/D0FD00079E, 2021

Christian, K.E., Brune, W.H., Mao, J. and Ren, X.: Global sensitivity analysis of GEOS-Chem modeled ozone and hydrogen oxides during the INTEX campaigns. Atmospheric Chemistry and Physics, 18(4), 2443–2460. https://doi.org/10.5194/acp-18-2443-2018, 2018

Christiansen, A., Mickley, L.J., Liu, J., Oman, L.D. and Hu, L.: Multidecadal increases in global tropospheric ozone derived from ozonesonde and surface site observations: can models reproduce ozone trends?. Atmospheric Chemistry and Physics, 22(22), 14751–14782. https://doi.org/10.5194/acp-22-14751-2022, 2022

Coker, E. and Kizito, S.: A narrative review on the human health effects of ambient air pollution in Sub-Saharan Africa: an urgent need for health effects studies. International journal of environmental research and public health, 15(3), 427. https://doi.org/10.3390/ijerph15030427, 2018

Crutzen, P.J., Grooß, J.U., Brühl, C., Müller, R. and Russell III, J.M.: A reevaluation of the ozone budget with HALOE UARS data: No evidence for the ozone deficit. Science, 268(5211), 705–708. https://doi.org/10.1126/science.268.5211.705, 1995

David, L.M. and Nair, P.R.: Diurnal and seasonal variability of surface ozone and NOx at a tropical coastal site: Association with mesoscale and synoptic meteorological conditions. Journal of Geophysical Research: Atmospheres, 116(D10). https://doi.org/10.1029/2010JD015076, 2011

David, L.M. and Ravishankara, A.R.: Boundary layer ozone across the Indian subcontinent: Who influences whom?. Geophysical Research Letters, 46(16), pp.10008-10014. https://doi.org/10.1029/2019GL082416, 2019

David, L.M., Ravishankara, A.R., Brewer, J.F., Sauvage, B., Thouret, V., Venkataramani, S. and Sinha, V.: Tropospheric ozone over the Indian subcontinent from 2000 to 2015: Data set and simulation using GEOS-Chem chemical transport model. Atmospheric Environment, 219, 117039. https://doi.org/10.1016/j.atmosenv.2019.117039, 2019

Deeter, M. N., Martínez-Alonso, S., Edwards, D. P., Emmons, L. K., Gille, J. C., Worden, H. M., Sweeney, C., Pittman, J. V., Daube, B. C., and Wofsy, S. C.: The MOPITT Version 6 product: algorithm enhancements and validation, Atmos. Meas. Tech., 7, 3623–3632, https://doi.org/10.5194/amt-7-3623-2014, 2014.

Deshmukh, D.K., Deb, M.K., Verma, D., Verma, S.K. and Nirmalkar, J.: Aerosol size distribution and seasonal variation in an urban area of an industrial city in Central India. Bulletin of environmental contamination and toxicology, 89, 1098–1104. https://doi.org/10.1007/s00128-012-0834-1, 2012

Devi, N.L., Kumar, A. and Yadav, I.C.: PM10 and PM2. 5 in Indo-Gangetic Plain (IGP) of India: Chemical characterization, source analysis, and transport pathways. Urban Climate, 33, 100663. https://doi.org/10.1016/j.uclim.2020.100663, 2020

Dhanurkar, T., Budamala, V. and Bhowmik, R.D.: Understanding the association between global forest fire products and hydrometeorological variables. Science of The Total Environment, 945, 173911. https://doi.org/10.1016/j.scitotenv.2024.173911, 2024

Dyson, J.E., Whalley, L.K., Slater, E.J., Woodward-Massey, R., Ye, C., Lee, J.D., Squires, F., Hopkins, J.R., Dunmore, R.E., Shaw, M. and Hamilton, J.F.: Impact of HO 2 aerosol uptake on radical levels and O 3 production during summertime in Beijing. Atmospheric Chemistry and Physics Discussions, 2022, 1–43. https://doi.org/10.5194/acp-23-5679-2023, 2022

Eastham, S. D., Weisenstein, D. K., and Barrett, S. R. H.: Development and evaluation of the unified tropospheric–stratospheric chemistry extension (UCX) for the global chemistry-transport model GEOS-Chem, Atmos. Environ., 89, 52–63, 2014.

Fairlie, D. T., Jacob, D. J., and Park, R. J.: The impact of transpacific transport of mineral dust in the United States, Atmos. Environ., 41, 1251–1266, 2007.

Feng, T., Bei, N., Huang, R.J., Cao, J., Zhang, Q., Zhou, W., Tie, X., Liu, S., Zhang, T., Su, X. and Lei, W.: Summertime ozone formation in Xi'an and surrounding areas, China. Atmospheric Chemistry and Physics, 16(7), 4323–4342. https://doi.org/10.5194/acp-16-4323-2016, 2016

682 Fiore, A.M., Jacob, D.J., Bey, I., Yantosca, R.M., Field, B.D., Fusco, A.C. and Wilkinson, J.G.: Background
683 ozone over the United States in summer: Origin, trend, and contribution to pollution episodes. Journal of
684 Geophysical Research: Atmospheres, 107(D15), ACH-11. https://doi.org/10.1029/2001JD000982, 2002

685 Fountoukis, C. and Nenes, A.: ISORROPIA II: a computationally efficient
686 thermodynamic equilibrium model for K+–Ca2+–Mg2+–NH4+–Na+–SO42−–NO3−–Cl−–
687 H2O aerosols, Atmos. Chem. Phys., 7, 4639–4659, https://doi.org/10.5194/acp-7-
688 4639-2007, 2007.

689 Fritz, T.M., Eastham, S.D., Emmons, L.K., Lin, H., Lundgren, E.W., Goldhaber, S., Barrett, S.R. and Jacob, D.J.:
690 Implementation and evaluation of the GEOS-Chem chemistry module version 13.1. 2 within the Community Earth
691 System Model v2. 1. Geoscientific Model Development, 15(23), pp.8669-8704., 2022.

692 Galbally, I.E. and Roy, C.R.: Destruction of ozone at the earth's surface. Quarterly Journal of the Royal
693 Meteorological Society, 106(449), 599–620. https://doi.org/10.1002/qj.49710644915, 1980

694 Gao, J., Wang, H., Liu, W., Xu, H., Wei, Y., Tian, X., Feng, Y., Song, S. and Shi, G.: Hydrogen peroxide serves
695 as pivotal fountainhead for aerosol aqueous sulfate formation from a global perspective. Nature Communications,
696 15(1), 4625. https://doi.org/10.1038/s41467-024-48793-1, 2024

697 Gao, J., Zhu, B., Xiao, H., Kang, H., Pan, C., Wang, D. and Wang, H.: Effects of black carbon and boundary layer
698 interaction on surface ozone in Nanjing, China. Atmospheric Chemistry and Physics, 18(10), 7081–7094.
699 https://doi.org/10.5194/acp-18-7081-2018, 2018

700 Gao, M., Gao, J., Zhu, B., Kumar, R., Lu, X., Song, S., Zhang, Y., Jia, B., Wang, P., Beig, G. and Hu, J.: Ozone
701 pollution over China and India: seasonality and sources. Atmospheric Chemistry and Physics, 20(7), 4399–4414.
702 https://doi.org/10.5194/acp-20-4399-2020 , 2020

703 Garg, A. and Gupta, N.C.: The great smog month and spatial and monthly variation in air quality in ambient air
704 in Delhi, India. https://doi.org/10.5696/2156-9614-10.27.200910, Journal of Health and Pollution, 10(27),
705 200910, 2020

706 George, I.J. and Abbatt, J.P.D.: Heterogeneous oxidation of atmospheric aerosol particles by gas-phase radicals.
707 Nature Chemistry, 2(9), 713–722. https://doi.org/10.1038/nchem.806, 2010

708 GEOS-Chem Support Team: Particulate matter in GEOS-Chem: PM2.5 / PM10 guide. GEOS-Chem Classic
709 14.6.3 documentation. Available at: https://geos-chem.readthedocs.io/en/latest/geos-chem-shared-
710 docs/supplemental-guides/pm25-pm10-guide.html

711 (Accessed: [20/12/2024]), 2023

712 Gerasopoulos, E., Kouvarakis, G., Vrekoussis, M., Donoussis, C., Mihalopoulos, N. and Kanakidou, M.:
713 Photochemical ozone production in the Eastern Mediterranean. Atmospheric Environment, 40(17), pp.3057-3069.
714 https://doi.org/10.1016/j.atmosenv.2005.12.061, 2006

Giglio, L., Randerson, J.T. and Van Der Werf, G.R.: Analysis of daily, monthly, and annual burned area using the fourth-generation global fire emissions database (GFED4). Journal of Geophysical Research: Biogeosciences, 118(1), pp.317-328. https://doi.org/10.1002/jgrg.20042, 2013

Ginoux, P., Prospero, J.M., Gill, T.E., Hsu, N.C. and Zhao, M.: Global-scale attribution of anthropogenic and natural dust sources and their emission rates based on MODIS Deep Blue aerosol products. Reviews of Geophysics, 50(3). https://doi.org/10.1029/2012RG000388, 2012

Gopikrishnan, G.S. and Kuttippurath, J.: Global tropical and extra-tropical tropospheric ozone trends and radiative forcing deduced from satellite and ozonesonde measurements for the period 2005–2020. Environmental Pollution, 361, 124869. https://doi.org/10.1016/j.envpol.2024.124869, 2024

Gopikrishnan, G.S., Kuttippurath, J., Raj, S., Singh, A. and Abbhishek, K.: Air quality during the COVID–19 lockdown and unlock periods in India analyzed using satellite and ground-based measurements. Environmental Processes, 9(2), 28. https://doi.org/10.1007/s40710-022-00585-9, 2022

Guenther, A.B., Jiang, X., Heald, C.L., Sakulyanontvittaya, T., Duhl, T.A., Emmons, L.K. and Wang, X.: The Model of Emissions of Gases and Aerosols from Nature version 2.1 (MEGAN2. 1): an extended and updated framework for modeling biogenic emissions. Geoscientific Model Development, 5(6), pp.1471-1492. https://doi.org/10.5194/gmd-5-1471-2012, 2012

Guil-López, R., Mota, N., Llorente, J., Millán, E., Pawelec, B., Fierro, J.L.G. and Navarro, R.M.: Methanol synthesis from CO2: a review of the latest developments in heterogeneous catalysis. Materials, 12(23), p.3902. https://doi.org/10.3390/ma12233902. 2019

Guttikunda, S. and Nishadh, K.A.: Evolution of India's PM 2.5 pollution between 1998 and 2020 using global reanalysis fields coupled with satellite observations and fuel consumption patterns. Environmental Science: Atmospheres, 2(6), 1502–1515. https://doi.org/10.1039/D2EA00027J, 2022

Hassan, M.A., Mehmood, T., Liu, J., Luo, X., Li, X., Tanveer, M., Faheem, M., Shakoor, A., Dar, A.A. and Abid, M.: A review of particulate pollution over Himalaya region: Characteristics and salient factors contributing ambient PM pollution. Atmospheric Environment, 294, 119472. https://doi.org/10.1016/j.atmosenv.2022.119472, 2023

Hoesly, R.M., Smith, S.J., Feng, L., Klimont, Z., Janssens-Maenhout, G., Pitkanen, T., Seibert, J.J., Vu, L., Andres, R.J., Bolt, R.M. and Bond, T.C.: Historical (1750–2014) anthropogenic emissions of reactive gases and aerosols from the Community Emissions Data System (CEDS). Geoscientific Model Development, 11(1), pp.369-408. https://doi.org/10.5194/gmd-11-369-2018, 2018

Horowitz, H.M., Jacob, D.J., Zhang, Y., Dibble, T.S., Slemr, F., Amos, H.M., Schmidt, J.A., Corbitt, E.S., Marais, E.A. and Sunderland, E.M.: A new mechanism for atmospheric mercury redox chemistry: implications for the global mercury budget. Atmospheric Chemistry and Physics, 17(10), pp.6353-6371, https://doi.org/10.5194/ACP-17-6353-2017, 2017

Hudman, R.C., Moore, N.E., Mebust, A.K., Martin, R.V., Russell, A.R., Valin, L.C. and Cohen, R.C.: Steps towards a mechanistic model of global soil nitric oxide emissions: implementation and space based-constraints. Atmospheric Chemistry and Physics, 12(16), pp.7779-7795. https://doi.org/10.5194/acp-12-7779-2012, 2012

Ivatt, P.D., Evans, M.J. and Lewis, A.C: Suppression of surface ozone by an aerosol-inhibited photochemical ozone regime. Nature Geoscience, 15(7), 536–540. https://doi.org/10.1038/s41561-022-00972-9, 2022

Jacob, D.J., Horowitz, L.W., Munger, J.W., Heikes, B.G., Dickerson, R.R., Artz, R.S. and Keene, W.C.: Seasonal transition from NOx-to hydrocarbon-limited conditions for ozone production over the eastern United States in September. Journal of Geophysical Research: Atmospheres, 100(D5), 9315–9324. https://doi.org/10.1029/94JD03125, 1995

Jacob, D.J.: Heterogeneous chemistry and tropospheric ozone. Atmospheric Environment, 34(12-14), 2131–2159. https://doi.org/10.1016/S1352-2310(99)00462-8**,** 2000

Jaeglé, L., Quinn, P. K., Bates, T. S., Alexander, B., and Lin, J.-T.: Global distribution of sea salt aerosols: new constraints from in situ and remote sensing observations, Atmos. Chem. Phys., 11, 3137–3157, https://doi.org/10.5194/acp-11-3137-2011, 2011.

Jayachandran, V. and Rao, T.N.: Long-term regional air pollution characteristics in and around Hyderabad, India: Effects of natural and anthropogenic sources. Atmospheric Environment: X, 22, 100254. https://doi.org/10.1016/j.aeaoa.2024.100254, 2024

Jia, M., Zhao, T., Cheng, X., Gong, S., Zhang, X., Tang, L., Liu, D., Wu, X., Wang, L. and Chen, Y.: Inverse relations of PM2. 5 and O3 in air compound pollution between cold and hot seasons over an urban area of east China. Atmosphere, 8(3), 59. https://doi.org/10.3390/atmos8030059, 2017

Kajino, M., Ishijima, K., Ching, J., Yamaji, K., Ishikawa, R., Kajikawa, T., Singh, T., Nakayama, T., Matsumi, Y., Kojima, K. and Patra, P.K.: Impact of post monsoon crop residue burning on PM 2.5 over North India: Optimizing emissions using a high-density in situ surface observation network. EGUsphere, 2024, 1–40. https://doi.org/10.5194/egusphere-2024-1811, 2024

Karambelas, A., Fiore, A.M., Westervelt, D.M., McNeill, V.F., Randles, C.A., Venkataraman, C., Pierce, J.R., Bilsback, K.R. and Milly, G.P.: Investigating drivers of particulate matter pollution over India and the implications for radiative forcing with GEOS-Chem-TOMAS15. Journal of Geophysical Research: Atmospheres, 127(24), e2021JD036195. https://doi.org/10.1029/2021JD036195, 2022

Kedia, S. and Ramachandran, S.: Seasonal variations in aerosol characteristics over an urban location and a remote site in western India. Atmospheric Environment, 45(12), 2120–2128. https://doi.org/10.1016/j.atmosenv.2011.01.040, 2011

Keller, C.A., Long, M.S., Yantosca, R.M., Da Silva, A.M., Pawson, S. and Jacob, D.J.: HEMCO v1. 0: A versatile, ESMF-compliant component for calculating emissions in atmospheric models. Geoscientific Model Development, 7(4), pp.1409-1417. https://doi.org/10.5194/gmd-7-1409-2014, 2014

Kim, J., Cho, H.K., Mok, J., Yoo, H.D. and Cho, N.: Effects of ozone and aerosol on surface UV radiation variability. Journal of Photochemistry and Photobiology B: Biology, 119, 46–51. https://doi.org/10.1016/j.jphotobiol.2012.11.007, 2013

Kim, P.S., Jacob, D.J., Fisher, J.A., Travis, K., Yu, K., Zhu, L., Yantosca, R.M., Sulprizio, M.P., Jimenez, J.L., Campuzano-Jost, P. and Froyd, K.D.: Sources, seasonality, and trends of southeast US aerosol: an integrated analysis of surface, aircraft, and satellite observations with the GEOS-Chem chemical transport model. Atmospheric Chemistry and Physics, 15(18), 10411–10433. https://doi.org/10.5194/acp-15-10411-2015, 2015

Koch, D., Schulz, M., Kinne, S., McNaughton, C., Spackman, J.R., Balkanski, Y., Bauer, S., Berntsen, T., Bond, T.C., Boucher, O. and Chin, M.: Evaluation of black carbon estimations in global aerosol models. Atmospheric Chemistry and Physics, 9(22), pp.9001-9026. https://doi.org/10.5194/acp-9-9001-2009, 2009

Kolb, C.E., Cox, R.A., Abbatt, J.P.D., Ammann, M., Davis, E.J., Donaldson, D.J., Garrett, B.C., George, C., Griffiths, P.T., Hanson, D.R. and Kulmala, M.: An overview of current issues in the uptake of atmospheric trace gases by aerosols and clouds. Atmospheric Chemistry and Physics, 10(21), 10561–10605. https://doi.org/10.5194/acp-10-10561-2010, 2010

Kumar, R., Barth, M.C., Nair, V.S., Pfister, G.G., Suresh Babu, S., Satheesh, S.K., Krishna Moorthy, K., Carmichael, G.R., Lu, Z. and Streets, D.G.: Sources of black carbon aerosols in South Asia and surrounding regions during the Integrated Campaign for Aerosols, Gases and Radiation Budget (ICARB). Atmospheric Chemistry and Physics, 15(10), pp.5415-5428. https://doi.org/10.5194/acp-15-5415-2015, 2015

Kumari, S., Radhadevi, L., Gujre, N., Rao, N. and Bandaru, M.: Assessing the impact of forest fires on air quality in Northeast India. Environmental Science: Atmospheres, 5(1), 82–93. https://doi.org/10.1039/D4EA00107A, 2025

Kutal, G., Kolhe, A., Mahajan, C., Varpe, S., Patil, R., Singh, P. and Aher, G.R.: Characteristics of Surface ozone levels at climatologically and topographically distinct Metropolitan cities in India. Asian Journal of Atmospheric Environment, 16(2), 2022004. https://doi.org/10.5572/ajae.2022.004, 2022

Kuttippurath, J., Abbhishek, K., Gopikrishnan, G.S. and Pathak, M.: Investigation of long–term trends and major sources of atmospheric HCHO over India. Environmental Challenges, 7, 100477. https://doi.org/10.1016/j.envc.2022.100477, 2022

Kuttippurath, J., Singh, A., Dash, S.P., Mallick, N., Clerbaux, C., Van Damme, M., Clarisse, L., Coheur, P.F., Raj, S., Abbhishek, K. and Varikoden, H.: Record high levels of atmospheric ammonia over India: Spatial and temporal analyses. Science of the Total Environment, 740, 139986. https://doi.org/10.1016/j.scitotenv.2020.139986, 2020

Lakey, P.S.J., Berkemeier, T., Baeza-Romero, M.T., Pöschl, U., Shiraiwa, M. and Heard, D.E. Towards a better understanding of the HO 2 uptake coefficient to aerosol particles measured during laboratory experiments. Environmental Science: Atmospheres, 4(7), 813-829, https://doi.org/10.1039/D4EA00025K,2024

Lakshmi, K.K., Nishanth, T., Kumar, M.S. and Valsaraj, K.T.: A comprehensive review of surface ozone variations in several indian hotspots. Atmosphere, 15(7), 852. https://doi.org/10.3390/atmos15070852, 2024

Lal, S., Venkataramani, S., Chandra, N., Cooper, O.R., Brioude, J. and Naja, M.: Transport effects on the vertical distribution of tropospheric ozone over western India. Journal of Geophysical Research: Atmospheres, 119(16), 10012–10026. https://doi.org/10.1002/2014JD021854, 2014

Lavanyaa, V.P., Harshitha, K.M., Beig, G. and Srikanth, R.: Background and baseline levels of PM2. 5 and PM10 pollution in major cities of peninsular India. Urban Climate, 48, 101407. https://doi.org/10.1016/j.uclim.2023.101407, 2023

Li, J., Chen, X., Wang, Z., Du, H., Yang, W., Sun, Y., Hu, B., Li, J., Wang, W., Wang, T. and Fu, P.: Radiative and heterogeneous chemical effects of aerosols on ozone and inorganic aerosols over East Asia. Science of the Total Environment, 622, 1327–1342. https://doi.org/10.1016/j.scitotenv.2017.12.041, 2018

Li, K., Jacob, D.J., Liao, H., Shen, L., Zhang, Q. and Bates, K.H.:. Anthropogenic drivers of 2013–2017 trends in summer surface ozone in China. Proceedings of the National Academy of Sciences, 116(2), 422-427. https://doi.org/10.1073/pnas.1812168116, 2019

Li, Q., Borge, R., Sarwar, G., de la Paz, D., Gantt, B., Domingo, J., Cuevas, C.A. and Saiz-Lopez, A.: Impact of halogen chemistry on summertime air quality in coastal and continental Europe: application of the CMAQ model and implications for regulation. Atmospheric Chemistry and Physics, 19(24), 15321–15337. https://doi.org/10.5194/acp-19-15321-2019, 2019

Li, X., Wang, W., Yang, S., Cheng, Y., Zeng, L., Yu, X., Lu, S., Liu, Y., Hu, M., Xie, S. and Huang, X.: Ozone sensitivity regimes vary at different heights in the planetary boundary layer. Science of The Total Environment, 944, p.173712. https://doi.org/10.1016/j.scitotenv.2024.173712, 2024

Li, Z., Guo, J., Ding, A., Liao, H., Liu, J., Sun, Y., Wang, T., Xue, H., Zhang, H. and Zhu, B.: Aerosol and boundary-layer interactions and impact on air quality. National Science Review, 4(6), pp.810-833. https://doi.org/10.1093/nsr/nwx117**,** 2017

Lin, J.T., Youn, D., Liang, X.Z. and Wuebbles, D.J.: Global model simulation of summertime US ozone diurnal cycle and its sensitivity to PBL mixing, spatial resolution, and emissions. Atmospheric Environment, 42(36), pp.8470-8483. https://doi.org/10.1016/j.atmosenv.2008.08.012, 2008

Logan, J.A.: Tropospheric ozone: Seasonal behavior, trends, and anthropogenic influence. Journal of Geophysical Research: Atmospheres, 90(D6), 10463–10482. https://doi.org/10.1029/JD090iD06p10463, 1985

Lokhande, S.V. and Khan, A.: Assessment of Impact of Vehicular Pollution on Ambient Air Quality A Case Study of Nagpur City. International Journal of Engineering Research & Technology (IJERT), 10(6). https://www.ijert.org/research/assessment-of-impact-of-vehicular-pollution-on-ambient-air-quality-a-case-study-of-nagpur-city-IJERTV10IS060206.pdf, 2021

Lu, H., Lyu, X., Cheng, H., Ling, Z. and Guo, H.: Overview on the spatial–temporal characteristics of the ozone formation regime in China. Environmental Science: Processes & Impacts, 21(6), 916–929. https://pubs.rsc.org/en/content/articlelanding/2019/em/c9em00098d, 2019

Lu, X., Zhang, L., Liu, X., Gao, M., Zhao, Y. and Shao, J.: Lower tropospheric ozone over India and its linkage to the South Asian monsoon. Atmospheric Chemistry and Physics, 18(5), 3101–3118. https://doi.org/10.5194/acp-18-3101-2018, 2018

Lucchesi, R.: File specification for GEOS-5 FP (Forward processing) (No. GSFC-E-DAA-TN19791). https://ntrs.nasa.gov/api/citations/20150001437/downloads/20150001437.pdf, 2013

Macintyre, H.L. and Evans, M.J.: Parameterisation and impact of aerosol uptake of HO 2 on a global tropospheric model. Atmospheric Chemistry and Physics, 11(21), 10965–10974. https://doi.org/10.5194/acp-11-10965-2011, 2011

Mahilang, M., Deb, M.K., Pervez, S., Tiwari, S. and Jain, V.K.: Biogenic secondary organic aerosol formation in an urban area of eastern central India: Seasonal variation, size distribution and source characterization. Environmental Research, 195, 110802. https://doi.org/10.1016/j.envres.2021.110802, 2021

Maji, S. and Sonwani, S.: Nature of Sand and Dust Storm in South Asian Region: Extremities and Environmental Impacts. In Extremes in Atmospheric Processes and Phenomenon: Assessment, Impacts and Mitigation (113–139). Singapore: Springer Nature Singapore. https://doi.org/10.1007/978-981-16-7727-4_6, 2022

Manisalidis, I., Stavropoulou, E., Stavropoulos, A. and Bezirtzoglou, E.: Environmental and health impacts of air pollution: a review. Frontiers in public health, 8, 14. https://doi.org/10.3389/fpubh.2020.00014, 2020

Mao, Y.H., Shang, Y., Liao, H., Cao, H., Qu, Z. and Henze, D.K.: Sensitivities of ozone to its precursors during heavy ozone pollution events in the Yangtze River Delta using the adjoint method. Science of the Total Environment, 925, 171585. https://doi.org/10.1016/j.scitotenv.2024.171585, 2024

Mhawish, A., Banerjee, T., Sorek-Hamer, M., Bilal, M., Lyapustin, A.I., Chatfield, R. and Broday, D.M.: Estimation of high-resolution PM2. 5 over the Indo-Gangetic Plain by fusion of satellite data, meteorology, and land use variables. Environmental Science & Technology, 54(13), 7891–7900. https://pubs.acs.org/doi/10.1021/acs.est.0c01769, 2020

Mills, G., Buse, A., Gimeno, B., Bermejo, V., Holland, M., Emberson, L. and Pleijel, H.: A synthesis of AOT40-based response functions and critical levels of ozone for agricultural and horticultural crops. Atmospheric Environment, 41(12), 2630–2643. https://doi.org/10.1016/j.atmosenv.2006.11.016, 2007

Misra, P., Takigawa, M., Khatri, P., Dhaka, S.K., Dimri, A.P., Yamaji, K., Kajino, M., Takeuchi, W., Imasu, R., Nitta, K. and Patra, P.K.: Nitrogen oxides concentration and emission change detection during COVID-19 restrictions in North India. Scientific Reports, 11(1), 9800. https://doi.org/10.1038/s41598-021-87673-2, 2021

Mogno, C., Palmer, P.I., Knote, C., Yao, F. and Wallington, T.J.: Seasonal distribution and drivers of surface fine particulate matter and organic aerosol over the Indo-Gangetic Plain. Atmospheric Chemistry and Physics, 21(14), 10881–10909. https://doi.org/10.5194/acp-21-10881-2021, 2021

NAAQS: Guidelines for the Measurement of Ambient Air Pollutants: Volume-II, https://cpcb.nic.in/openpdffile.php?id=UHVibGljYXRpb25GaWxlLzk5OV8xNzM1NjIyNTA0X21lZGlhcGhvdG8xNjkzMC5wZGY=, 2023

Namdeo, P., Chakraborty, T.C. and Chakraborty, A.: Two decades of aerosol trends over India: seasonal characteristics and urban-rural dynamics. Environmental Research Letters, 19(12), 124065. https://doi.org/10.1088/1748-9326/ad9291, 2024

Nilaya, M., Vaibhavi, V., Agrawal, S. and Gupta, L.: Analysing the anomalous relationship between precipitation and PM10 concentrations in Peninsular India. In E3S Web of Conferences (Vol. 559, 04011). EDP Sciences. https://doi.org/10.1051/e3sconf/202455904011, 2024

Pai, S.J., Heald, C.L., Coe, H., Brooks, J., Shephard, M.W., Dammers, E., Apte, J.S., Luo, G., Yu, F., Holmes, C.D. and Venkataraman, C.: Compositional constraints are vital for atmospheric PM2. 5 source attribution over India. ACS earth and space chemistry, 6(10), pp.2432-2445. https://pubs.acs.org/doi/10.1021/acsearthspacechem.2c00150, 2022

Pandya, S., Gadekallu, T.R., Maddikunta, P.K.R. and Sharma, R.: A study of the impacts of air pollution on the agricultural community and yield crops (Indian context). Sustainability, 14(20), 13098. https://doi.org/10.3390/su142013098, 2022

Park, R. J.: Natural and transboundary pollution influences on sulfate-nitrate-ammonium aerosols in the United States: Implications for policy, J. Geophys. Res., 109, 13791, https://doi.org/10.1029/2003JD004473, 2004.

Pathak, M. and Kuttippurath, J.: Air quality trends in rural India: analysis of NO 2 pollution using satellite measurements. Environmental Science: Processes & Impacts, 24(12), 2437–2449. https://doi.org/10.1039/D2EM00293K, 2022

Pathak, M. and Kuttippurath, J.: Elucidating the changing particulate matter pollution and associated health effects in rural India during 2000–2019. Environmental Pollution, 348, 123830. https://doi.org/10.1016/j.envpol.2024.123830, 2024

Patil, S.D., Preethi, B., Bansod, S.D., Singh, H.N., Revadekar, J.V. and Munot, A.A.: On the association between pre-monsoon aerosol and all-India summer monsoon rainfall. Journal of Atmospheric and Solar-Terrestrial Physics, 102, 1–7. https://doi.org/10.1016/j.jastp.2013.04.006, 2013

Paulot, F., Naik, V. and W. Horowitz, L.: Reduction in Near-Surface Wind Speeds With Increasing CO2 May Worsen Winter Air Quality in the Indo-Gangetic Plain. Geophysical Research Letters, 49(18), e2022GL099039. https://doi.org/10.1029/2022GL099039, 2022

Payra, S., Gupta, P., Sarkar, A., Bhatla, R. and Verma, S.: Changes in tropospheric ozone concentration over Indo-Gangetic Plains: the role of meteorological parameters. Meteorology and Atmospheric Physics, 134(6), 96. https://doi.org/10.1007/s00703-022-00932-3, 2022

Phanikumar, D.V., Kumar, K.N., Bhattacharjee, S., Naja, M., Girach, I.A., Nair, P.R. and Kumari, S.: Unusual enhancement in tropospheric and surface ozone due to orography induced gravity waves. Remote Sensing of Environment, 199, 256–264. https://doi.org/10.1016/j.rse.2017.07.011, 2017

Pye, H. O. T., Chan, A. W. H., Barkley, M. P., and Seinfeld, J.H.: Global modeling of organic aerosol: the importance of reactive nitrogen (NOx and NO3), Atmos. Chem. Phys., 10, 11261–11276, doi:10.5194/acp-10-11261-2010, 2010.

Ramachandran, S. and Cherian, R.: Regional and seasonal variations in aerosol optical characteristics and their frequency distributions over India during 2001–2005. Journal of Geophysical Research: Atmospheres, 113(D8). https://doi.org/10.1029/2007JD008560, 2008

Rathore, A., Gopikrishnan, G.S. and Kuttippurath, J.: Changes in tropospheric ozone over India: Variability, long-term trends and climate forcing. Atmospheric Environment, 309, 119959. https://doi.org/10.1016/j.atmosenv.2023.119959, 2023

Romer, P.S., Duffey, K.C., Wooldridge, P.J., Edgerton, E., Baumann, K., Feiner, P.A., Miller, D.O., Brune, W.H., Koss, A.R., De Gouw, J.A. and Misztal, P.K.: Effects of temperature-dependent NO x emissions on continental ozone production. Atmospheric Chemistry and Physics, 18(4), 2601–2614.https://doi.org/10.5194/acp-18-2601-2018, 2018

Saikia, A.: The Burning Issue: Why it's so urgent to stop burning agricultural residues in the Indo-Gangetic Plain and Himalayan Foothills of South Asia. https://blog.icimod.org/clean-air/the-burning-issue-why-its-so-urgent-to-stop-burning-agricultural-residues-in-the-indo-gangetic-plain-and-himalayan-foothills-of-south-asia/, 2025

Saini, D., Lataye, D. and Motghare, V.: Studies on the variation in concentrations of respirable suspended particulate matter (PM10), NO2 and SO2 in and around Nagpur. MAUSAM, 74(3), 761–786. https://doi.org/10.54302/mausam.v74i3.828, 2023

Salvermoser, M.J., Kogelschatz, U. and Murnick, D.E.: Influence of humidity on photochemical ozone generation with 172 nm xenon excimer lamps. The European Physical Journal Applied Physics, 47(2), p.22812. https://doi.org/10.1051/EPJAP%2F2009063, 2009

Santra, P., Kumar, S. and Roy, M.M.: Thar Desert: Source for dust storm. In Natural hazards (233–252). CRC Press.
https://www.taylorfrancis.com/chapters/edit/10.1201/9781315166841-11/thar-desert-priyabrata-santra-suresh-kumar-roy, 2018

Sen, A., Abdelmaksoud, A.S., Ahammed, Y.N., Banerjee, T., Bhat, M.A., Chatterjee, A., Choudhuri, A.K., Das, T., Dhir, A., Dhyani, P.P. and Gadi, R.: Variations in particulate matter over Indo-Gangetic Plains and Indo-

Himalayan Range during four field campaigns in winter monsoon and summer monsoon: role of pollution pathways. Atmospheric environment, 154, 200–224. https://doi.org/10.1016/j.atmosenv.2016.12.054, 2017

Shaeb, K.H.B.: Aerosol Studies over Central India. Hydrocarbon Pollution and its Effect on the Environment, 31–51.https://books.google.com/books?hl=en&lr=&id=ekr9DwAAQBAJ&oi=fnd&pg=PA31&dq=Shaeb,+K.H.B.,+2019.+Aerosol+Studies+over+Central+India.+Hydrocarbon+Pollution+and+its+Effect+on+the+Environment,+pp.31-51.&ots=U9Y_oEHL2X&sig=FObpjLDIDDxhe_zkavqM4Pm44-Y, 2019

Sheehy, P.M., Volkamer, R., Molina, L.T. and Molina, M.J.: Oxidative capacity of the Mexico City atmosphere–Part 2: A RO x radical cycling perspective. Atmospheric Chemistry and Physics, 10(14), 6993–7008. https://doi.org/10.5194/acp-10-6993-2010, 2010

Sicard, P., Khaniabadi, Y.O., Leca, S. and De Marco, A.: Relationships between ozone and particles during air pollution episodes in arid continental climate. Atmospheric Pollution Research, 14(8), 101838. https://doi.org/10.1016/j.apr.2023.101838, 2023

Singh, N., Banerjee, T., Raju, M.P., Deboudt, K., Sorek-Hamer, M., Singh, R.S. and Mall, R.K.: Aerosol chemistry, transport, and climatic implications during extreme biomass burning emissions over the Indo-Gangetic Plain. Atmospheric Chemistry and Physics, 18(19), 14197–14215. https://doi.org/10.5194/acp-18-14197-2018, 2018

Singh, T., Matsumi, Y., Nakayama, T., Hayashida, S., Patra, P.K., Yasutomi, N., Kajino, M., Yamaji, K., Khatri, P., Takigawa, M. and Araki, H.: Very high particulate pollution over northwest India captured by a high-density in situ sensor network. Scientific Reports, 13(1), 13201. https://doi.org/10.1038/s41598-023-39471-1, 2023

Sinha, B. and Sinha, V.: Source apportionment of volatile organic compounds in the northwest Indo-Gangetic Plain using a positive matrix factorization model. Atmospheric Chemistry and Physics, 19(24), 15467–15482. https://doi.org/10.5194/acp-19-15467-2019, 2019

Sinha, V., Kumar, V. and Sarkar, C.: Chemical composition of pre-monsoon air in the Indo-Gangetic Plain measured using a new air quality facility and PTR-MS: high surface ozone and strong influence of biomass burning. Atmospheric Chemistry and Physics, 14(12), 5921–5941. https://doi.org/10.5194/acp-14-5921-2014, 2014

Sivaprasad, P. and Babu, C.A.: Seasonal variation and classification of aerosols over an inland station in India. Meteorological applications, 21(2), 241–248. https://doi.org/10.1002/met.1319, 2014

Song, H., Lu, K., Dong, H., Tan, Z., Chen, S., Zeng, L. and Zhang, Y.: Reduced aerosol uptake of hydroperoxyl radical may increase the sensitivity of ozone production to volatile organic compounds. Environmental Science & Technology Letters, 9(1), 22–29. https://doi.org/10.1021/acs.estlett.1c00893, 2021

Song, Z., Wang, M. and Yang, H.: Quantification of the impact of fine particulate matter on solar energy resources and energy performance of different photovoltaic technologies. ACS Environmental Au, 2(3), 275–286. https://doi.org/10.1021/acsenvironau.1c00048, 2022

Stavrakou, T., Müller, J.F., Boersma, K.F., Van Der A, R.J., Kurokawa, J., Ohara, T. and Zhang, Q.: Key chemical NO x sink uncertainties and how they influence top-down emissions of nitrogen oxides. Atmospheric Chemistry and Physics, 13(17), 9057–9082. https://doi.org/10.5194/acp-13-9057-2013, 2013

Travis, K.R. and Jacob, D.J.: Systematic bias in evaluating chemical transport models with maximum daily 8 h average (MDA8) surface ozone for air quality applications: a case study with GEOS-Chem v9. 02. Geoscientific Model Development, 12(8), 3641–3648. https://doi.org/10.5194/gmd-12-3641-2019, 2019

UNESCAP: Key Initiatives of Government of India on "Low Carbon Transport." (n.d.). https://www.unescap.org/sites/default/d8files/event-documents/16%20Key%20Initiatives%20on%20Low%20Carbon%20Transport%2C%20India.pdf, 2022

Usmani, M., Kondal, A., Wang, J. and Jutla, A.: Environmental association of burning agricultural biomass in the Indus River basin. GeoHealth, 4(11), e2020GH000281. https://doi.org/10.1029/2020GH000281, 2020

Wang, K., Kang, S., Lin, M., Chen, P., Li, C., Yin, X., Hattori, S., Jackson, T.L., Yang, J., Liu, Y. and Yoshida, N.: Himalayas as a global hot spot of springtime stratospheric intrusions: Insight from isotopic signatures in sulfate aerosols. Research in Cold and Arid Regions, 16(1), 5–13. https://doi.org/10.1016/j.rcar.2024.03.002, 2024

Wang, L., Qin, K. and Zhao, B.: Spatiotemporal variations in the association between PM2. 5 and ozone in the yangtze river economic belt: Impacts of meteorological and emissions factors. Atmospheric Environment, 329, 120534. https://doi.org/10.1016/j.atmosenv.2024.120534, 2024

Wang, P., Chen, Y., Hu, J., Zhang, H. and Ying, Q.: Attribution of tropospheric ozone to NO x and VOC emissions: considering ozone formation in the transition regime. Environmental science & technology, 53(3), 1404–1412. https://doi.org/10.1021/acs.est.8b05981, 2018

Wang, W., Li, X., Shao, M., Hu, M., Zeng, L., Wu, Y. and Tan, T.: The impact of aerosols on photolysis frequencies and ozone production in Beijing during the 4-year period 2012–2015. Atmospheric Chemistry and Physics, 19(14), 9413–9429. https://doi.org/10.5194/acp-19-9413-2019, 2019

Wang, X., Jacob, D. J., Eastham, S. D., Sulprizio, M. P., Zhu, L., Chen, Q., Alexander, B., Sherwen, T., Evans, M. J., Lee, B. H., Haskins, J. D., Lopez-Hilfiker, F. D., Thornton, J. A., Huey, G. L., and Liao, H.: The role of chlorine in global tropospheric chemistry, Atmos. Chem. Phys., 19, 3981–4003, https://doi.org/10.5194/acp-19-3981-2019, 2019.

Wang, Y., Gao, W., Wang, S., Song, T., Gong, Z., Ji, D., Wang, L., Liu, Z., Tang, G., Huo, Y. and Tian, S.: Contrasting trends of PM2. 5 and surface-ozone concentrations in China from 2013 to 2017. National Science Review, 7(8), 1331–1339. https://doi.org/10.1093/nsr/nwaa032, 2020

Wu, W., Ge, Y., Wang, Y., Su, J., Wang, X., Zhou, B. and Chen, J.: Vertical ozone formation mechanisms resulting from increased oxidation on the mountainside of Mount Tai, China. PNAS nexus, 3(9), p.pgae347. https://doi.org/10.1093/pnasnexus/pgae347, 2024

Xing, J., Wang, J., Mathur, R., Wang, S., Sarwar, G., Pleim, J., Hogrefe, C., Zhang, Y., Jiang, J., Wong, D.C. and Hao, J.: Impacts of aerosol direct effects on tropospheric ozone through changes in atmospheric dynamics and photolysis rates. Atmospheric Chemistry and Physics, 17(16), 9869–9883. https://doi.org/10.5194/acp-17-9869-2017, 2017

Yadav, R., Vyas, P., Kumar, P., Sahu, L.K., Pandya, U., Tripathi, N., Gupta, M., Singh, V., Dave, P.N., Rathore, D.S. and Beig, G.: Particulate Matter Pollution in Urban Cities of India During Unusually Restricted Anthropogenic Activities. Frontiers in Sustainable Cities, 4, 792507. https://doi.org/10.3389/frsc.2022.792507, 2022

Yang, L.H., Jacob, D.J., Colombi, N.K., Zhai, S., Bates, K.H., Shah, V., Beaudry, E., Yantosca, R.M., Lin, H., Brewer, J.F. and Chong, H. Tropospheric NO 2 vertical profiles over South Korea and their relation to oxidant chemistry: implications for geostationary satellite retrievals and the observation of NO2 diurnal variation from space. Atmospheric Chemistry and Physics, 23(4), 2465-2481. https://doi.org/10.5194/acp-23-2465-2023, 2023

Yu, W., Ye, T., Zhang, Y., Xu, R., Lei, Y., Chen, Z., Yang, Z., Zhang, Y., Song, J., Yue, X. and Li, S.: Global estimates of daily ambient fine particulate matter concentrations and unequal spatiotemporal distribution of population exposure: a machine learning modelling study. The Lancet Planetary Health, 7(3), e209–e218. https://www.thelancet.com/journals/lanplh/article/PIIS2542-5196(23)00008-6/fulltext, 2023

Zhang, L., Jacob, D.J., Downey, N.V., Wood, D.A., Blewitt, D., Carouge, C.C., van Donkelaar, A., Jones, D.B., Murray, L.T. and Wang, Y: Improved estimate of the policy-relevant background ozone in the United States using the GEOS-Chem global model with 1/2× 2/3 horizontal resolution over North America. Atmospheric Environment, 45(37), 6769–6776. https://doi.org/10.1016/j.atmosenv.2011.07.054, 2011

Zhang, X., Xiao, X., Wang, F., Yang, Y., Liao, H., Wang, S. and Gao, M.: Discordant future climate-driven changes in winter PM2. 5 pollution across India under a warming climate. Elementa: Science of the Anthropocene, 11(1). https://doi.org/10.1525/elementa.2022.00149, 2023

Zhao, K., Yuan, Z., Wu, Y., Huang, J., Yang, F., Zhang, X., Huang, D. and Jiang, R.: Identification of synergistic control for ozone and PM2. 5 pollution during a large-scale emission reduction in China. Atmospheric Research, 295, 107025. https://doi.org/10.1016/j.atmosres.2023.107025, 2023

Zhu, L., Jacob, D.J., Eastham, S.D., Sulprizio, M.P., Wang, X., Sherwen, T., Evans, M.J., Chen, Q., Alexander, B., Koenig, T.K. and Volkamer, R.: Effect of sea salt aerosol on tropospheric bromine chemistry. Atmospheric Chemistry and Physics, 19(9), pp.6497-6507. https://doi.org/10.5194/acp-19-6497-2019, 2019

Zou, J., Sun, J., Ding, A., Wang, M., Guo, W. and Fu, C.: Observation-based estimation of aerosol-induced reduction of planetary boundary layer height. Advances in Atmospheric Sciences, 34(9), pp.1057-1068. https://doi.org/10.1007/s00376-016-6259-8, 2017